Effect of Extrusion on the Electrical, Mechanical and Rheological Properties of an Ethylene Butylacrylate/Carbon Black/Graphite Nanoplatelets Nanocomposite

by

Elena Álvarez Díez

Diploma work No. 134/2014
at Department of Materials and Manufacturing Technology
CHALMERS UNIVERSITY OF TECHNOLOGY
Gothenburg, Sweden

Diploma work as an Erasmus exchange student 134/2014

Performed at: Department of Materials and Manufacturing Technology
Chalmers University of Technology, SE – 41296 Gothenburg

Examiner: Professor Mikael Rigdahl
Department of Materials and Manufacturing Technology
Chalmers University of Technology, SE – 41296 Gothenburg

Supervisor: Doctor Ruth Ariño Mariné
Department of Materials and Manufacturing Technology
Chalmers University of Technology, SE – 41296 Gothenburg

Effect of Extrusion on the Electrical, Mechanical and Rheological Properties of an Ethylene Butylacrylate/Carbon Black/Graphite Nanoplatelets Nanocomposite

Elena Alvarez Díez

Diploma work no 134/2014
Department of Materials and Manufacturing Technology
Chalmers University of Technology
SE-41296 Gothenburg
Sweden

CHALMERS Reproservice

Gothenburg, Sweden 2014

Effect of Extrusion on the Electrical, Mechanical and Rheological Properties of an Ethylene Butylacrylate/Carbon Black/Graphite Nanoplatelets Nanocomposite

Elena Álvarez Díez
Department of Materials and Manufacturing Technology
Chalmers University of Technology

Abstract

The possibility of introducing graphite nanoplatelets (GNP) in a *semiconductive polymeric composite** filled with carbon black (CB) through the extrusion mixing was studied, the application being the semiconductive screens in high voltage direct current extruded cables.

An appropriate extrusion processing aiming for adequate semiconductive properties of the extruded material was searched for. The possible detrimental effect by adding GNP and CB on the mechanical and rheological properties of the material was also studied. The influence of different processing variables was examined through the application of two different extrusion temperatures (160°C and 180°C), two rotation screw speeds (50 rpm and 100 rpm) and two types of screw (barrier screw and conventional screw).

Materials with 3.5, 5 and 12 volumen-% of hybrid filler content were analyzed, the hybrid filler consisting of 80 weight-% GNP and 20 weight-% CB. Direct current measurements were performed in order to determine the electrical conductivity. Scanning electron microscopy and X-ray diffraction were used for characterizing the morphology and the structure of the fillers and composites. Uniaxial tensile tests and viscosity measurements with a capillary viscometer were conducted in the study of the mechanical and rheological properties, respectively.

The results showed a beneficial effect on the electrical properties with the introduction of GNP. The reason could be a synergistic effect between the two fillers due to the geometries of the fillers. The best results regarding the electrical properties were obtained with the conventional screw, showing lower percolation thresholds than those observed with the barrier screw. A possible de-agglomeration and low breakage of the GNP obtained with the conventional screw whereas high breakage of GNP with the barrier screw could be the reasons for the observation. No significant differences in the electrical properties were observed when changing the extrusion temperatures and screw speeds. In addition, an acceptable melt viscosity and stiffness was achieved at the filler contents studied.

**Semiconductive polymeric composite*: composite that uses a polymer as matrix (in this work ethyl butyl-acrylate) and conductive particles such as carbon black as filler.

Key words: semiconductive polymeric composite, hybrid conductive filler, graphite nanoplatelets, carbon black, extrusion mixing, barrier screw, conventional screw, synergistic effect

Contents

NOMENCLATURE ..... **I**
1. INTRODUCTION **1**
2. BACKGROUND **4**
2.1. MATERIALS 4
2.1.1. Ethylene butyl acrylate copolymer (EBA) *4*
2.1.2. Carbon black (CB) *5*
2.1.3. Graphite nanoplatelets (GNP) *6*
2.2. NANOCOMPOSITE BEHAVIOR THEORIES FOR CONDUCTIVITY 7
2.2.1. Percolation theory *7*
2.2.2. Synergistic effect *9*
2.2.3. Rheological properties *9*
2.2.4. Mechanical properties *10*
2.3. PROCESSING TECHNIQUES 11
2.3.1. Fundamentals of compounding *11*
2.3.2. Internal mixer *12*
2.3.3. Extrusion mixing *12*
2.3.4. Compounding variables *17*
2.3.5. Capillary rheometer *17*
2.4. CHARACTERISATION TECHNIQUES 19
2.4.1. Electrical properties *19*
3. EXPERIMENTAL **20**
3.1. RAW MATERIALS 20
3.2. PERCOLATION CURVE DETERMINATION 21
3.3. METHODS 22
3.3.1. Compounding of masterbatches *23*
3.3.2. Extrusion experiments *23*
3.3.3. Verification of filler content (TGA) *25*
3.3.4. Electrical measurements (two-point measuring technique) *26*
3.3.5. Morphological characterization of composite material and fillers (SEM and Optical Microscopy) *27*
3.3.6. Structural analysis of GNP (XRD) *28*
3.3.7. Uniaxial tensile tests *28*
3.3.8. Rheological measurements (Capillary Viscometer) *28*
4. RESULTS AND DISCUSION **29**
5. CONCLUSIONS **45**

Appendix A **47**
References **51**

Acknowledgements

First I would like to express my gratitude to my supervisor Ruth Ariño for her excellent guidance throughout this thesis and for having shared all her knowledge and time with me. I would also like to thank my examiner Mikael Rigdahl for having offered me the opportunity to carry out this thesis and for his time and precious supervision.

Second, the department of Materials and Manufacturing Technology are thanked for giving me the opportunity to work with them and for the treatment received. Thanks to Borealis AB and Swerea Group for providing the materials and sharing their equipment for the development of this thesis.

Thanks to all my friends, colleagues and staff at the department of Materials and Manufacturing Technology for the friendly atmosphere and time we shared.

Particularly I thank Raquel de Oro Calderón for always having the time to help me, Sujith Guru for being a magnificent opponent in the defense of this thesis and Mahesh V Sudaram for his time, knowledge and advice.

Finally, I would like to thank my family for the support received during my whole life, the education I have received and my brother César Luis Álvarez for always advising me and helping with his knowledge.

Nomenclature

Symbols

c	Percolation threshold	[Vol%]
P	Pressure	[Pa]
V	Velocity	[m/s]
D	Diameter	[m]
L	Length	[m]
E	Young´s Modulus	[Pa]
σ_b	Ultimate Strength	[Pa]
ε_b	Final Elongation	[%]
σ	Conductivity	[S/m]
τ_a	Apparent shear stress	[Pa]
μ_a	Apparent viscosity	[Pa·s]
γ_a	Apparent shear rate	[s^{-1}]

Acronyms

CB	Carbon Black
CNT	Carbon Nanotubes
EBA	Ethyl Butyl Acrylate
EG	Expanded Graphite
GIC	Graphite Intercalation Compound
GNP	Graphite Nanoplatelets
HVAC	High Voltage Alternating Current
HVDC	High Voltage Direct Current
SEM	Scanning Electron Microscope
TGA	Thermogravimetric Analysis
Vol %	Volume percentage
Wt %	Weight percentage
XRD	X-ray Diffraction

Introduction

High voltage direct current cables (HVDC cables) have aroused great interest in the recent years. The continuous growth in energy consumption has pushed the electricity grid into a new challenge. Nowadays, large amounts of energy need to be carried for large distances in a globalized world. Because of their capacitive and inductive limitations, high voltage alternating current cables (HVAC cables) are not suitable for the present transmission grid. HVDC are widely used since they do not present any capacitive or inductive effects and they also provide advantages when linking asynchronous systems preventing cascading failures. Despite of their different functioning, both types of cables have a similar structure. Figure 1 shows a typical structure of an extruded HVDC cable. [1]

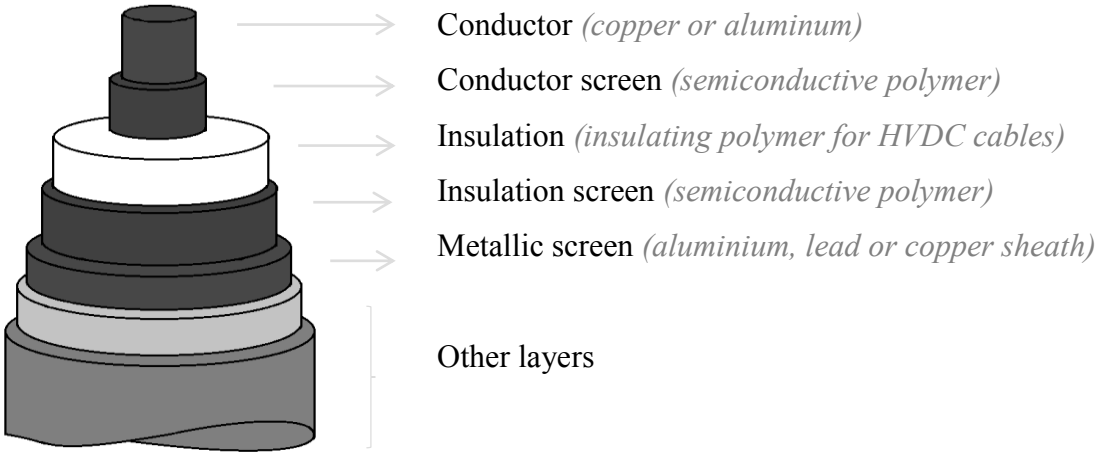

Figure 1. Structure of an extruded HVDC cable

In HVDC cables, two semiconductive* screen layers are required. The inner one is called *conductor screen* or *conductor shield* and the outer one *insulation screen* or *insulation shield*. Coextrusion is the manufacturing process used for cables with voltages up to 300kV and powers up to 1000MW. In this process, conductor shield, insulation, insulation screen and metallic screen are extruded around the conductor. [1]

The main function of the *conductor shield* is to provide a smooth, continuous and void-free interface between the conductor and the insulation as well as contribute to a homogenous radial electric field. Gaps of air, together with voltage differences, can produce electrical discharges (also called corona discharges) that may deteriorate the insulation. In addition, it is important to provide a homogeneous radial electric field in the insulation to avoid stresses that can damage the insulation. An analogous function applies to the *insulation screen*, in this case working between the insulation and the metallic screen layers. The presence of these two layers reduces premature failures and increases the lifetime. [1]

Therefore the materials used for these applications require on one hand some conductivity (to avoid high voltage differences at the interfaces) and on the other hand compatibility with the insulation (to be attached closely to the insulation). The cable standards demand a volume resistivity for the conductor shield below 100000 Ω·cm at 90°C and 130°C for continuous and emergency operating conditions respectively. In the case of the insulator shield the limiting requirement is 50000 Ω·cm at 90°C for

continuous operation temperature and 110°C as emergency conditions [2]**.** Composites with ethylene copolymers as matrix material and carbon black (CB) as conductive filler are the materials most widely used. In order to achieve the required conductivity, the amount of filler often needs to be between 25 and 40 weight percent (wt %). This high loading is a drawback for the manufacturing process due to the viscosity increase as well as for the mechanical properties, decreasing the flexibility [3]. Furthermore, a decrease in the amount of CB used would be preferred for material cost savings.

In previous studies, a synergistic effect on the electrical conductivity by replacing part of the CB by graphite nanoplatelets (GNP) was observed, with the best results for the hybrid systems consisting of 80 wt % GNP and 20 wt % CB [4] (see appendix A, Figure 35). The measured conductivities overcome those of the composites filled with CB or GNP separately.

It is believed that by modifying different parameters in the extrusion process, GNP could be further exfoliated or de-agglomerated (as has been observed with layered silicate platelets when extruded in a polymeric matrix, Figure 2) [5] resulting in a higher electrical conductivity. Besides the GNP exfoliation/de-agglomeration, a suitable orientation and dispersion of the filler is also desired and particle fragmentation should be avoided to some extent. In this work, the effect of extrusion mixing on the electrical and mechanical properties was studied. Morphological and rheological studies were also performed.

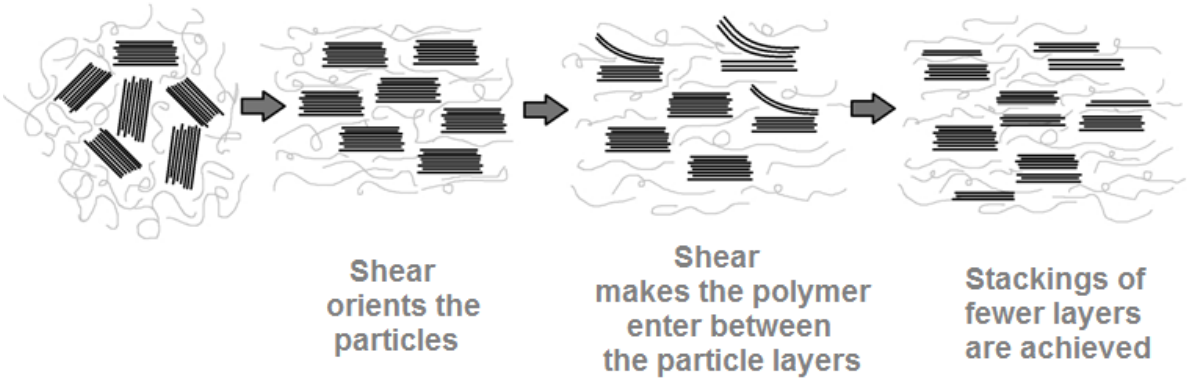

Figure 2. Effect of extrusion in filled polymer with layered silicate platelets.

Aim of this work

The aim of this work is to study the influence of extrusion on a polymer nanocomposite with ethylene butylacrylate as the matrix and carbon black and graphite nanoplatelets as the conducting fillers, with particular regard to the electrical conductivity of the material and, to a lesser extent, its mechanical properties and viscosity. The study will include case studies of different processing temperatures, screw speeds and types of screw.

Special attention will be paid to the analysis of a possible exfoliation or de-agglomeration of the graphite nanoplatelets on account of the recent interest in industrial processes to obtain single layers of graphite, i.e. graphene.

*In this thesis, semiconductive material is defined as a material with conductivity between that of the conductor and that of the insulator of high voltage cables. It is not referred to N-type or P-type nonlinear resistive materials.

1. Background

This chapter introduces the materials used in this work and provides an understanding of the theories that describe the performance of filled polymers with regard to electrical, mechanical and rheological properties. The processing techniques used and the effect of the different processing techniques and parameters on the material are also presented. An overview of the influential parameters is given for this reason. Finally, the basics for some characterization techniques used are given at the end of the chapter.

1.1. Materials

1.1.1. Ethylene butyl acrylate copolymer (EBA)

In this work, an ethylene butyl acrylate copolymer (EBA), also called ethylene n-butyl acrylate (EnBA) or poly (ethylene co-butyl acrylate) was used as a matrix material. This copolymer is composed of randomly arranged ethylene and butyl acrylate monomer units. [6] Figure 3 shows its structure.

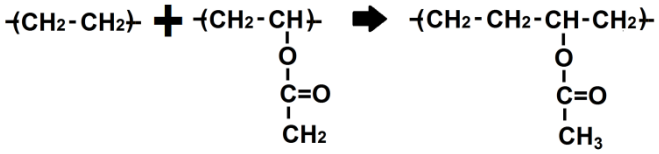

Figure 3 Polymerization and structure of ethyl butyl acrylate

EBA belongs to the copolymer group of acrylates, which together with the acetates are the common polymers used for semiconductive screens. Acrylates have better thermal stability than acetates, which in this case is of a great importance since not only higher temperatures in the extrusion process increase the production rate but the polymer must resist the heating from the cross-linking of the insulation (260-300°C).[3]

EBA is polymerized by the same high-pressure process as low-density polyethylene (LDPE) [7]. Although it is a thermoplastic it can be crosslinked by peroxide addition and applying heat and pressure. With this, the physical and heat resistant properties are improved without impairing other essential properties. [8] In cable manufacturing, crosslinking takes place after the cable leaves the co-extruder head [3].

The amount of acrylate monomers as well as the presence of fillers affect the crystallinity of the copolymer [9], [10]. The acrylic acid units reduce the crystallinity [9] whereas fillers may impede the crystallization process of EBA [10]. The crystalline regions constitute very compact structures and therefore, the presence of fillers in these regions is inhibited, creating regions with high amounts of fillers. In the case of conductive fillers, as in this work, this can contribute to a higher conductivity of the material [10].

In copolymers, the melting and glass transition temperatures depend on the weight fractions of monomers [11]. EBA has a melting point between 95 and 115°C, increasing as the butyl acrylate content decreases [12].

Other characteristics of EBA copolymers are good flexibility and additive compatibility what makes it suitable for highly filled compounds [13]. In addition, EBA exhibits a certain polarity, caused by the

butylester side groups [14] that increases the conductivity of the polymer [12], [15] and can improve the affinity to the fillers as has been observed with expanded graphite (EG) [16].

1.1.2. Carbon black (CB)

Carbon black was chosen as one of the components of the hybrid system. It is electrically conducting and widely used in polymer matrix composites for different applications [17]. It exists in the form of aciniform aggregates (the smallest dispersible unit) formed of spheroidal particles of elemental carbon [17], [18]**.** The size of the particles varies between 15 and 75 nm whereas for the aggregates it varies from 50 to 400 nm. Furthermore aggregates tend to collapse in agglomerates with a size between 100 and 1000 nm [19]. Figure 4 shows agglomerates of the carbon black used in this work. The particles' microstructure however is not well understood. Paracrystalline domains where planes of graphite lay in a turbostratic* stacking have been found [20]. For the graphitic structures, graphite plates with an interplane distance deviating from the expected have been observed by X-Ray diffraction [17]. In the center of the particles a lack of order in the structure is suspected [17].

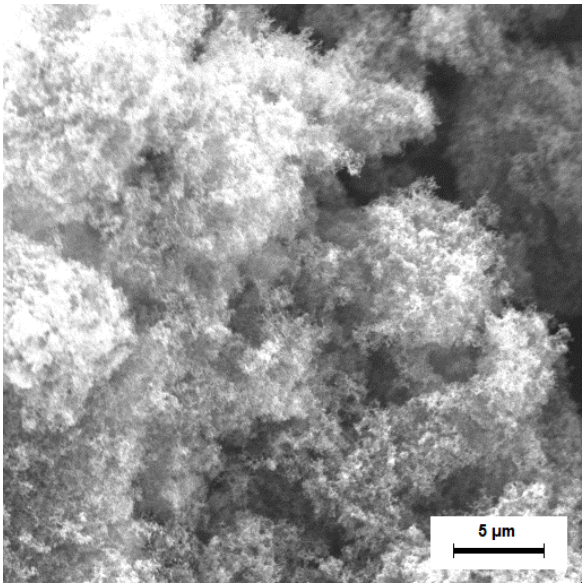

Figure 4 Carbon black agglomerates ENSACO 260G

Carbon black is obtained from the partial combustion or thermal decomposition of hydrocarbons [21] usually through the furnace process (from petrochemical or carbochemical origin) or the acetylene process (from acetylene gas) [17].

The conductivity of carbon black varies between 10^{-1} and 10^{2} $(\Omega \cdot cm)^{-1}$. Carbon black grades with high specific volumes, high structures and absence of impurities or chemical groups are preferred for conducting filled polymers. In addition, because porosity in carbon black increases the specific volume, higher porosity affects positively the conductivity of the material. High structured carbon, i.e. with larger number of particles per aggregates and branched sides, gives higher conductivity when added to a polymer although the specific volume is decreased [17]. This apparent contradiction is attributed to small particles, as in the case of high structured carbon blacks, that tend to aggregate and form agglomerates which can enhance the electrical properties.

Among the main drawbacks of carbon black, health concerns must be considered with caution [21]. The International Agency for Research on Cancer (IARC) has classified it in the Group 2B, carcinogens. Other drawbacks, especially when added in large amounts to a polymer matrix, are the increase of viscosity and the detrimental effect on mechanical properties such as flexibility [18].

**Turbostratic stacking of graphene sheets: random stacking that can be observed in many carbon materials in contrast to the regular stacking of the graphite structure* [22].

1.1.3. Graphite nanoplatelets (GNP)

GNP is a type of carbon-based nanoparticle in the form of platelets. These platelets are stacks of graphene sheets building up aggregates 2-15 nm thick with diameters between the sub-micron range and 50 μm. [23] As a result, the GNP particles have high aspect ratios and large surface areas.

At the atomic level, graphene layers are one atom thick layer of carbon atoms, each of them sp2–hybridized and forming three covalent bonds with the adjacent carbon atoms. The atoms form a lattice of hexagons in each graphene sheet and the sheets are bonded to each other by weak van der Waals forces. Consequently, highly anisotropic properties are obtained [24].

The high aspect ratio and large surface area of GNPs promote the formation of an electrically conductive network at lower filler contents than in the case of conventional carbon black (CB) [25]. GNP also enhances the barrier properties, thermal conductivity, the surface of the matrix polymers and mechanical properties such as the stiffness or the strength [23]**.**

GNP can be obtained by intercalation and delamination of natural graphite flakes. Atoms, ions or molecules known as intercalants can be intercalated between the parallel graphene layers giving as a result the graphite intercalation compound (GIC). The intercalants are based on strong oxidizing acids, such as sulfuric and nitric acids and metal chlorides. Vapor transport or thermal method, chemical oxidation and electrochemical methods are the typical techniques used for the intercalation. Once the intercalants are introduced between the graphene sheets, high temperatures are applied (typically 1050°C for 30s) expanding the GIC along the thickness direction by thermal shock and decomposition of the intercalants. The graphite layers are separated, the resulting material being called expanded graphite (EG). This is a porous worm rod material with weak bonds in its structure. The graphite nanoplatelets (GNP) are obtained through ultrasonication of the EG in a solvent, first breaking down the bonds of the EG flakes and after delamination giving smaller particles as a result. [24]

In some investigations EG has been used as the filler for conducting polymer applications. The electrical conductivity of EG-filled polymers is two orders of magnitude higher than obtained with GNP showing at the same time poorer mechanical properties. However, composites with GNP have lower percolation thresholds due to the higher aspect ratio of GNP. [24]

GNPs have been observed to easy agglomerate due to strong interplatelet van der Waals attractions and the high surface energy. CB has been successfully introduced into GNPs/epoxy resin composites [25], obtaining not only improved dispersion of GNP in the matrix, but also having a significant effect on the formation of the conductive network in the composite.

1.2. Nanocomposite behavior theories for conductivity

1.2.1. Percolation theory

The theoretical basis when studying the electrical properties of a polymer filled with conductive particles is the percolation theory. It describes the relation between the direct current conductivity of the material and the formation of a network of the conductive filler particles in the matrix. [26] When a low amount of conductive particles is added to the polymer matrix, the electrical current cannot pass through the composite. The reason is that the particles cannot form sufficient conductive pathways. If the amount of conductive particles is increased, the network formation may be enhanced until the number of paths is sufficient for the conductivity to experience a strong increase. At higher amounts of conductive particles, the increase in number of paths has a small effect on the conductivity and therefore the conductivity is stabilized. The representation of this effect in a plot relating the conductivity and the concentration of filler is shown in Figure 5 also known as the percolation curve. The volume fraction of conductive filler at which the conductivity experiences a sharp increase is called the percolation threshold (ϕ_c) In some filled polymers more than one percolation threshold have been observed. The percolation threshold and the electrical conductivity achieved are the main properties when describing electrical properties of conductive polymer composites. [27]

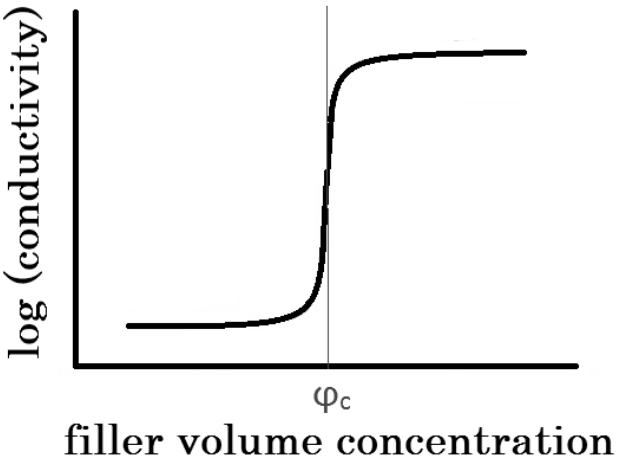

Figure 5 Percolation curve

The electrical conduction is the result of mainly two combined effects: the particle-particle contact and the tunneling effect. The mechanism of tunneling effect is the flow of electrons between conductive particles separated by the polymer less than a certain distance. [28] Dielectric breakdown and field emission are two other effects that can contribute to the electrical conductivity [24].

The percolation threshold and the electrical conductivity of the composite are influenced by the nature of the components as well as the processing and operating conditions. The aspect ratio and the shape of the filler, its orientation, dispersion and distribution within the polymer, the intrinsic electrical conductivity of the components and the crystallinity of the polymer are just some of the aspects that govern the electrical properties of the composite. [27] Unbounded gaps and micro-voids may also affect the electrical properties being highly resistant to electrical conduction and hindering the formation of the conductive network [24].

The effects of the mentioned aspects that affect the electrical properties in a filled polymer are summarized in Table 1.

Table 1. Effect on the electrical properties of different features in filled polymers.

Factor	Effect
Shape and size of the filler	Higher aspect ratio contribute with the movement of electrons and enhance the tunneling effect. Lower percolation threshold can therefore be achieved with this type of particles. In addition, asymmetrical fillers such as GNP contribute to into directionally dependent electrical properties. In general, with ellipsoidal particles as GNP the percolation threshold decreases with larger the diameter and increases linearly with the increasing thickness [29], [30]. In this work two different morphologies of filler have been used and their effect is studied separately. Spherical particles can increase the percolation threshold if the diameter is increased, the reason being the increased distance between particles provided that filler content is constant. CB cannot be considered completely spherical but aciniform. The structure is beneficial for the electrical properties for eliminating interfaces with the polymer and forming conductive networks.
Orientation of filler in the matrix	When anisotropic particles are introduced as fillers, the orientation has been observed to affect the percolation threshold. The alignment of particles in a parallel arrange is thought to hinder the contact between particles and percolation threshold is therefore increased.
Dispersion or de-agglomeration* of filler	The dispersion of aggregates may affect the aspect ratio and size of the filler. The effect of dispersion must therefore be studied from the point of view of aspect ratio and size variations.
Distribution* of filler in the matrix	The effect of higher distributions of fillers is a bigger distance between particles what leads to a more difficult network formation and therefore to higher percolation thresholds.
Polymer crystallinity	The crystalline regions of a polymer can contribute to the formation of conductive networks. The explanation is the particles preference to leave the crystalline regions enhancing the formation of the continuous conductive paths. The crystal

	morphology as well as the number and size of spherulites are also aspects to consider here. Lower percolation threshold are obtained with large but few spherulites. Slow cooling rate promotes the formation of such a crystal morphology.

There are theoretical models to predict the percolation threshold and conductivity as a function of the mentioned factors. The models by Kirkpatrick, Zallen and McLachlan, Mamunya et al. or Nielsen are just some of them. The limitations of these models are linked to the difficulties to consider all the aspects that affect these properties. [27]

However the effect of an hybrid filler as that used in this work has never been considered in these models. Different shapes of filler particles have been observed to introduce a synergistic effect with regard to the electrical properties of the composites, see below.

Dispersion or deagglomeration of filler: reduction in size of the agglomerates* [31].** *In the particular case of stackings of graphene sheets the term exfoliation can also be used.*
**Distribution of filler: spread of the filler in the polymeric matrix* [31].

1.2.2. Synergistic effect

A synergistic effect relating to the electrical properties has been observed when different conductive fillers are combined in a polymer matrix. Carbon nanotubes (CNT) with short carbon fibers [32], CNT with CB [33] [34], CNT, CB and GNP [35] or CB with GNP [25], are just some of the systems that have shown synergistic effects when combined. For examples, it has been observed that CB particles linked CNTs together resulting in the formation of more efficient networks. In addition, the CB particles also enhanced the ductility and fracture toughness of the filled polymer while retaining the high flexural modulus and strength [33].

In the work by Oxfall et al. [4], the synergistic effects with the hybrid filler CB-GNP (with high and low structured CB) was studied in composites, with EBA matrix, produced by melt mixing. The lowest percolation thresholds and highest conductivity values were found for hybrid fillers with a GNP-content between 70 and 80 wt % of the total filler content. Again, the formation of more efficient networks due to the bridging of CB between the GNP particles was suggested. The lower aspect ratio of CB allows a better dispersion in the matrix and bridges between rich areas of GNP are formed. At the same time the CB particles are thought to restrict the reagglomeration of GNP.

1.2.3. Rheological properties

Among the rheological properties of a polymer composite, the viscosity is the one of the most important parameters for processing [36]. Polymers exhibit a non-Newtonian behavior and it is well known that the viscosity of a polymer is affected by the introduction of fillers. Several models have been proposed to predict the viscosity of filled polymer composites. Einstein's equation for example describes the viscosity considering the volume fraction of filler incorporated [31]:

$$\eta = \eta_0 \cdot (1 + 0.67 \cdot f \cdot c + 1.62 \cdot f \cdot c^2) \quad \text{(I)}$$

Where η is the viscosity of the filled polymer, η_0 is the viscosity of the neat polymer, f is a geometrical factor equal to the ratio between the length and diameter of the filler particles ($f=\frac{L}{D}$) and c is the volume fraction of filler.

In this work, the shear viscosity of the filled polymer melt was measured with a capillary rheometer. The shear viscosity depends on several parameters such as the type of polymer, the size, concentration, shape, distribution and surface character of the filler and the affinity polymer-filler. The presence of additives in the melt can also modify the viscosity of the composite. [31], [36]

Both the particle size and the shape have a strong effect on the viscosity. Small particle size can lead to the formation of interphases which results in an increased viscosity. Mixing fine and coarse particles can result in a viscosity reduction, the reason being the intercalation of fine particles between the coarser particles increasing the packing ability of the particles. [36] The viscosity of suspensions filled with ellipsoid particles increases sharply with increasing aspect ratio. The Einstein model accounts for the effect of the particle shape on the viscosity through the Einstein parameter shown in equation (I) [36].

A more homogeneous filler distribution decreases the viscosity of a filled polymer. On the contrary, the formation of networks (structurization) in the melt increases the viscosity of the material and hampers its processability [36].

Due to enhanced friction forces between the filler and the matrix polymer and the increase of apparent particle concentration when layers of inert liquid are trapped on the filler surface, rough particles can increase the viscosity of a filled polymer [31].

Finally, the viscosity can be affected by the affinity between particles and polymer; higher affinity can lead to higher viscosities [31]. The addition of coupling agents can modify the affinity between the components. These additives as well as other such as surfactants, dispersants or lubricants can also affect the rheological properties of a suspension [31].

1.2.4. Mechanical properties

The mechanical properties of a given polymer are, as is well known, affected by the addition of fillers. The reinforcing effect depends on several factors such as the physical properties of the filler, the interaction filler-polymer, the amount of filler and the shape, size and distribution of the filler [31], [36]. For example, the effect of graphite on the mechanical properties is more pronounced than that of the CB [37]**.** In general, rigid fillers are suitable to improve the stiffness of the polymer while elastic particles are recommended for toughness improvement [31]. Graphite is one of the materials with very high stiffness per unit weight, with graphene sheets having a Young's modulus of 1600 GPa [37]. GNP has therefore the potential of being a high strengthening and stiffening filler.

Usually the polymer used as matrix e.g. EBA, has a low stiffness and strength and is fairly tough and extensible to transmit the load to the filler. High cohesive and interfacial shear strength are however required in the matrix in order for the filler to bear the stresses applied [31], [36]. The interface region is therefore an important factor to consider and a strong interface is required in order to increase strength and stiffness of the material. A weak interface may increase the toughness through a controlled debonding. [31] The interfacial strength can be improved by a good wetting of the filler, friction given by the filler surfaces and chemical reactions between matrix and filler. Filler particles with irregular surfaces offer higher friction with the matrix although the wetting properties are depressed compared to particles with smooth surfaces. Water and contaminants can create layers around the filler lowering the adhesion matrix-polymer. In order to improve the adhesion, surface treatments of the fillers may be required. [31]

Large surface areas of the filler particles are in general beneficial for strength and stiffness. GNP with a high aspect ratio has a big surface area. An increased surface area however, can result in in filler agglomeration which is detrimental for the strength and impact resistance. Contrary, the modulus may increase with increasing amounts of agglomerates. [31] The graphite sheets are fragile and when broken the reinforcing properties are negatively affected. Compounding methods should avoid an excessive breakage of the particle. [37] Higher amounts of filler, which also means larger surface area, will give higher stiffness and sometimes higher strength but an excessive number of particles may increase the probability of agglomerates. Similarly, a small particle size may also contribute to the reinforcement of the matrix. [31]

The orientation of particles must be considered with regards to the mechanical properties since GNP has anisotropic properties [24].

Finally, the addition of hard filler may lead to a loss of elastic properties of the polymeric matrix as well as the reduction of polymer swell. The elongation at break of graphite-filled polymers is generally lower than that of the unfilled polymer. [31]

1.3. Processing techniques

In order to compound fillers with polymers, different techniques are available. These can be classified as discontinuous techniques (*more flexible but with problems of batch to batch variations*) or continuous techniques (*consistent techniques although subject to a reliable feeding and take off equipment*). Within the batch wise systems internal mixers are the most common. However, continuous compounding techniques have been increasingly adopted by the industry, especially extrusion mixing due to its consistency. In the case of the cable industry, extrusion mixing has been adopted for the production of semiconductive screens. As done in this work, internal mixers are frequently used for preliminary studies. Afterwards, extrusion mixing was performed with different type of screws in a single screw extruder such as barrier single screw and conventional single screw in order to analyze their effect on the material studied. All these compounding techniques, together with the twin screw mixer used for masterbatch compounding and the capillary rheometer also used for processing in this work are introduced in this section. [31]

1.3.1. Fundamentals of compounding

Compounding is a technique for the preparation of filled polymer systems where polymers are softened, melted and intermingled with solid fillers and/or other liquid additives to form the mixed system. Usually, four steps take place during a compounding process: incorporation of fillers in the polymer matrix, wetting of the fillers by the polymer, dispersion of the agglomerates and distribution of the filler. The process starts with the incorporation of the materials through the feeding system and the wetting of filler by the polymer. The surface chemistry of both filler and polymer (i.e. inorganic vs organic character as in the case of GNP and CB in EBA) can hinder the wetting features, forming as a result agglomerates and voids around the clusters. The shear forces during the mixing process may then breakdown the agglomerates and disperse the fillers in the matrix. [31]

Different compounding techniques, however, apply shear forces to different extents. In this work their effect on the fillers was studied in order to obtain the best electrical properties.

1.3.2. Internal mixer

The internal mixer is a batch compounding technique where the mixing action is performed by two rotors that rotate inside a cavity called mixing chamber. The form of the materials introduced in the mixing chamber is usually powder or granulates. Figure 6 shows a schematic drawing of the internal mixer used in this work. The capacity of the mixing chamber determines the amount of material in a batch. The turning of the rotors can be done in the same (co-rotating) or opposite directions (counter-rotating). Also, the rotation speed of the rotors can be the same or different depending on the friction forces desired. However, the rotation speeds can vary during the mixing process. [31]

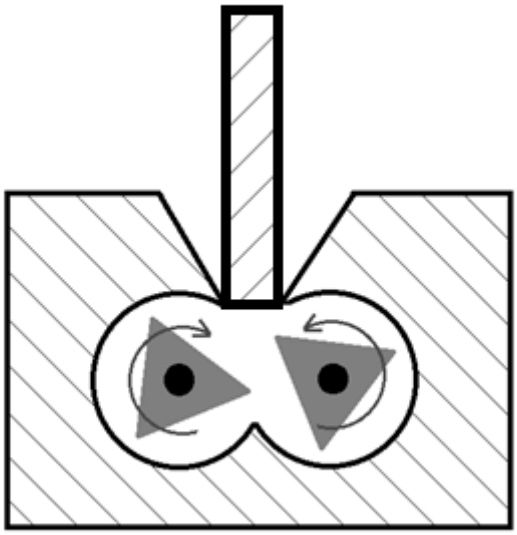

Figure 6. Cross section of an internal mixer chamber

Three types of mixing can be observed in an internal mixer: [31]

- The dispersive mixing that is mainly observed on the tips of the rotor blades.
- The extensive mixing that is a consequence of the shear and extensional flow that are observed between the walls of the chamber and the rotors and between the rotors tips in the entrance of the chamber.
- The distributive mixing that takes place due to the bulk convention in the chamber.

In this case, good mixing and not excessive breakages of filler could be expected.

There is a number of possible designs for the rotors blades that provide different levels of shear during the compounding. Sigma, Roller, Cam or Banbury types are just some of them [38]. The sigma type provides a high level of shear being therefore preferred for preparing filled polymer composites. However, the Cam type used in this work has showed the lower degree of dispersion [39].

1.3.3. Extrusion mixing

Among the continuous compounding techniques, extrusion mixing in particular offers high product quality and uniformity combined with high production volumes. Being an automatized mixing method, the possibilities of human errors are minimized and the batch–to-batch variation is eliminated. Another advantage is the close control on the shear energy introduced.[31]

Extrusion mixing offers a number of design possibilities from single-screw to twin screw extruders as well as additional equipment units that achieve a variety of end products. The desired properties of the end product, the production rate, economical aspects and the requirement of in-house or custom compounding are the main aspects that decide the type of extruder used. [31]

Single screw

The single screw extruder is the simplest of the extrusion mixers available. The material in a single screw passes in order through the feeding, melting and metering zones and leaves the extruder through the die. In a single screw extruder, frictional forces between the barrel (external cylinder where the screw is located) and the polymer are the responsible for carrying the polymer towards the die. However, these forces must overcome the friction forces between the screw and the polymer in order to move the material. Figure 7 shows a diagram of a single screw extruder.[31]

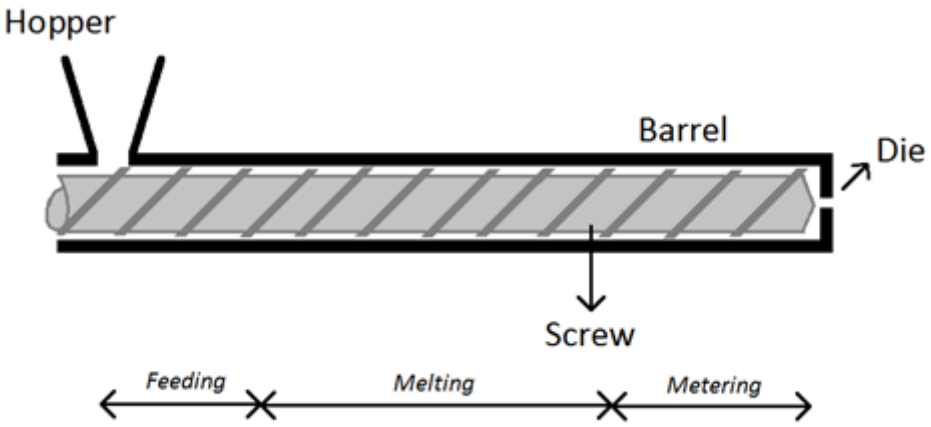

Figure 7. Diagram of a single screw extruder

The addition of the materials to the extruder is usually done through a conical hopper. The gravity forces as well as the particle-particle and particle-wall friction forces influence the rate at which the material is added to the extruder, sometimes introducing discontinuities in the feeding. However, special hoppers to control the feeding rates are available. [31]

After feeding, the material is melted in the melting zone of the extruder. Heat generated from the frictional forces and the heating system together with the pressure generated with the screw assist the polymer melting. A melt pool of polymer is formed on the leading edges of the screw flights. However, the solid bed of material needs time to melt and therefore very long screws are required; lengths to diameter of approximately 30:1 are common. [31]

Among the single screw extruder, the **conventional screw** provides the simplest design. The functioning of the conventional screw is simple and can be simplified to the melting of the material and the pumping of material towards regions of higher pressure. Figure 8 and 9 show the conventional screw used in this work and a detail of the flights on the screw, respectively. [31]

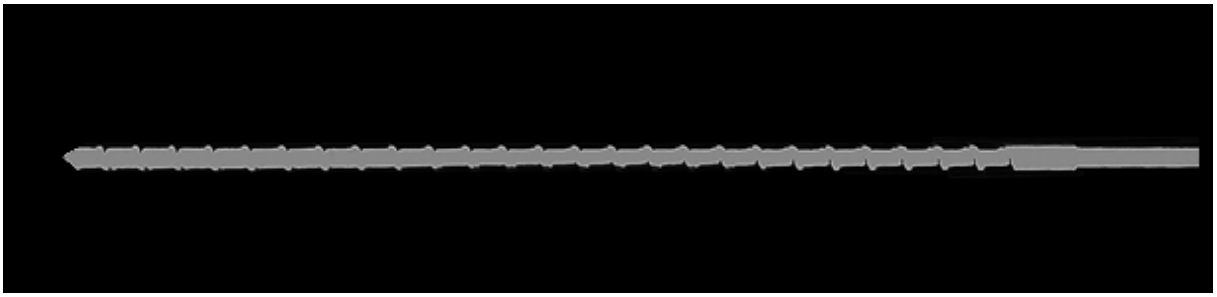

Figure 8. Conventional screw used in this work

Figure 9. Detail of the ending part of the conventional screw used in this work.

The mixing action takes place in the metering zone of the extruder. The shear forces mix the material and moves it towards the die along a spiral path through the screw channel. However, the fact that the movement of the material through the extruder and the mixing action are derived from the same shearing action limits the degree of mixing in the conventional single screw. [31]

In a conventional screw, the fillers are oriented parallel to the bottom of the channel regardless of the initial orientation. Consequently, the mixing action achieved in single screw extruders is generally poor. [31]

Alternatives to the conventional screw are usually considered when enhanced mixing is required. Mixing devices are usually incorporated in the screw. An example of these mentioned devices is the second flights extending over the length of the screw that can be observed in the **Maillefer screw**. Figure 10 shows a picture of the Maillefer screw used in this work where the mentioned second flights can be observed. [40]

Figure 10. Second flights of the Maillefer single screw used in this work

Additional distribution can be achieved by the incorporations of distributive or dispersive mixing elements that split the flow of material into several channels and combine them afterwards. The Saxton

distributor is an example of these additional distributive devices. [41] Figures 11 and 12 show the Maillefer screw used in this work and the Saxton distributor incorporated at the end of this, respectively.

The effect on the rupture or breakage of added particles has also been studied in a previous work using cellulose fibers in a polymeric matrix. A higher degree of breakage of the fibers was observed when compounding the material with the Maillefer screw extruder and a Saxton distributor integrated than with the conventional screw extruder [42].

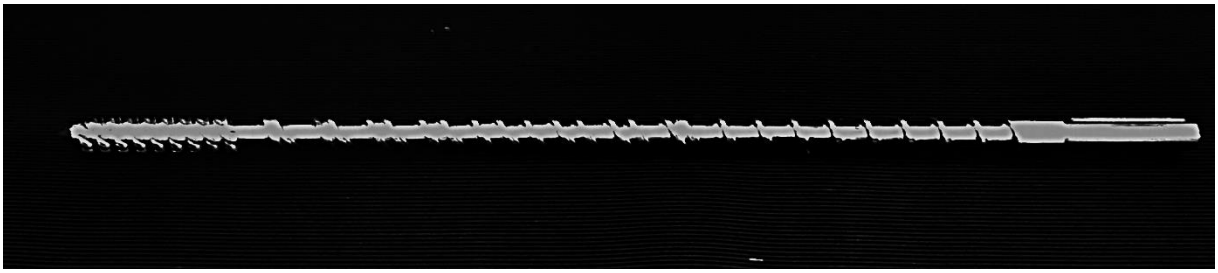

Figure 11. Maillefer single screw used in this work

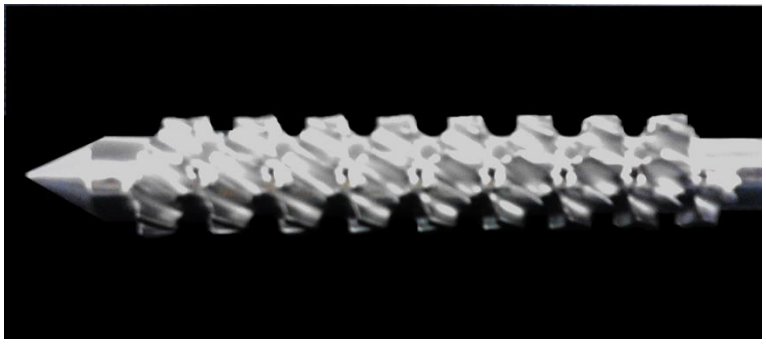

Figure 12. Saxton distributor

The achievable level of dispersion of fillers with a single screw is however limited. Improvements in filler dispersion can be achieved only by powerful shear forces. In this direction, the speed can be increased to intensify mixing although an increase in the energy input can lead to excessive temperatures and therefore the speed is usually limited to 100-150 rpm. When better mixing is required, the twin screw extruders should be considered. [31]

Twin screw extruders

Twin screw extruders were developed to overcome some of the limitations of single screw extruders. Different types of twin screw offer different abilities for distributive and dispersive mixing depending on the desired product properties. [31]

The two main classifications for twin screws are related to the relative position between the screws and the direction of rotation. Intermeshing screws are those whose distance between the screws is smaller than their major diameter. Consequently the rest of cases are called non-intermeshing screws. Besides, screws rotating in the same direction are called co-rotating screws whereas counter-rotating screws are those that rotate in opposite directions. Figure 13 illustrates the mentioned twin screws configurations.

The selection between the different types must be done according to the particular application. For many filling operations however, the co-rotating systems are preferred for process flexibility. [31]

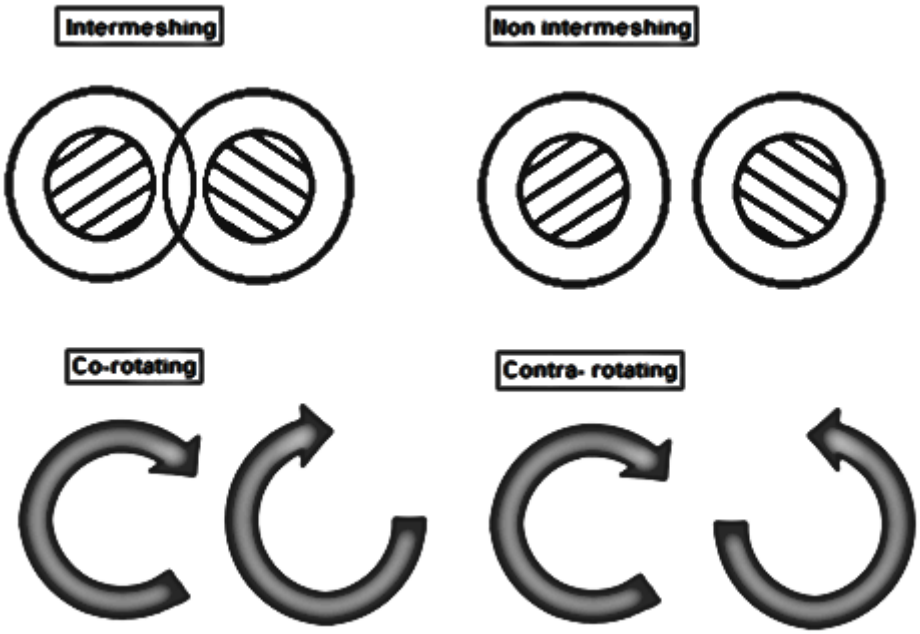

Figure 13 Twin screw configurations.

The co-rotating intermeshing twin-screw extruder was used in this work. This configuration, with the channel of one screw intruding into the other and the screws rotating in the same direction provides a positive pumping displacement. In addition, a better homogenization and dispersion of the material is achieved by the co-rotating screws due to a back and forth movement between the screws. [31]

However, the mixing in the axial direction cannot be attained with the twin screw extruder and therefore the materials must be mixed at the moment of their incorporation. The flow pattern describing an 8 between the two screws ensures an earlier and more complete melting in a relatively short distance. The desired degree of mixing in the twin screw extruder is achieved with less mechanical energy input and, therefore, less heat is introduced in the material. [31]

The screws can be designed for balancing the pumping and mixing characteristics. Short screw elements and special kneading elements of various widths are used to build up the screw with the desired shear intensities. By selecting different numbers of flights, the intensity of the shearing action can be changed. [31]

The effect on the breakage has also been studied in a previous work using cellulose fibers in a polymeric matrix. A higher breakage of the fibers was observed when compounding the material with the twin screw extruder than with single screw extruders [43].

1.3.4. Compounding variables.

A number of factors affect the final quality of the product with regards to by the level of dispersion in the melt state with a certain compounding technique. The mixer system, mixing time, rotor speed and mixing temperature are just some of these influential factors. The effect of these factors are often difficult to determine due to the strong interactions between them. In the case of the internal mixer the pressure used in the chamber, the chamber loading and the order in which the materials are added have influence the dispersion. [31]

As explained above, each mixing equipment develops different shear stress and therefore provides different dispersion of the filler, a better dispersion often being achieved with the twin screw extruder. In addition to the effect on dispersion, the type of mixer can also affect the oxidative degradation of the material if the residence times are excessively long. The twin screw, for example, avoids significant degradation thanks to its shorter residence times. [31]

An increased screw rotational speed introduces higher shear strains and deformations in the material resulting in a further breakage of the agglomerates (although not very effective). However, increased screw speeds also lead to more air entrapment. Usually, the screw speed is chosen to obtain a balance between these two effects being at the same time limited by the heat generation. [31]

Regarding the effect on the dispersion, the temperature during compounding should be considered. Higher temperatures reduce the viscosity of the materials resulting in lower shear stress and thus lower degree of dispersive mixing. On the other hand, the wetting characteristics of the polymer are improved with temperature increases. Therefore, in order to obtain the optimum dispersion the temperature during the compounding process must be balanced. [31]

Finally, in the case of the internal mixer, the breakage of agglomerates is enhanced and the number of voids diminished when higher pressures are used. In addition, high loadings of the mixing chamber can result in a lack of dispersion whereas low chamber loadings may not develop the stresses required for the correct mixing. The degree of mixing is affected also by the order of incorporation of the fillers and matrix to the mixing chamber. [31]

1.3.5. Capillary rheometer

In this work, a capillary rheometer was used to produce some specimens and to measure the viscosity of the filled polymers.

A capillary rheometer consists of three elements: the reservoir, the plunger and the capillary die. The reservoir is a metal cylinder with a heating system where the polymer is introduced and melted. Then the plunger moves down and pushes the polymer towards the capillary die. The polymer passes through the capillary with a specific diameter and length. When the polymer leaves the capillary die it swells in the air and solidifies forming the extrudate. Figure 14 shows a schematic drawing of a capillary rheometer.[31]

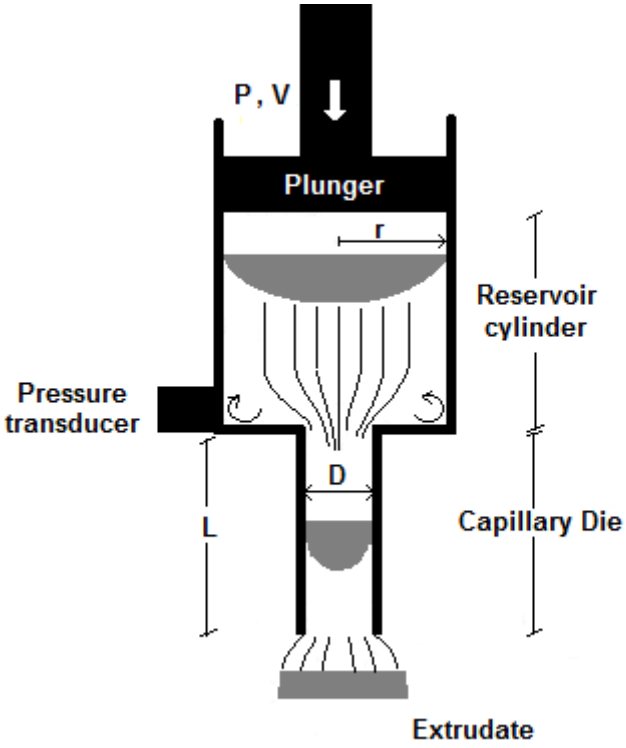

Figure 14 Schematic drawing of a capillary rheometer

The diameters of the capillary die are usually between 0.5 and 2 mm and the ratio between the length and diameter are between 5 and 50. The common capillary rheometers can provide shear rates from 1 to 100000 s^{-1}.

The flow within the capillary rheometer must be considered when polymers are filled with particles. Within the capillary a velocity gradient is at hand with higher speed in center of the tube because of the friction against the walls (higher shear stress on these regions). When the polymer contains filler particles, these try to move from the walls of the tube towards the center where lower stresses are present. Therefore a lower filler concentration should be expected close to the surfaces of the extrudate. The effect is especially important with large filler particles and when high shear rates are achieved. [31]

The viscosity was calculated from the volume flow rate and the pressure drop through the capillary. For that purpose there is a force transducer that measures the pressure in the lower part of the reservoir. The volume flow rate is calculated from the speed of the plunger and the diameter of the reservoir.

Volume flow rate and pressure drops are measured at different shear rates and then an approximation for the viscosity is calculated from the relation between the apparent shear stress and shear rate as follows:

$$\text{Apparent shear stress} = \tau_a = \Delta P \cdot R^2 \cdot L \quad \text{(II)}$$

$$\text{Apparent shear rate} = \gamma_a = 4 \cdot Q \cdot \pi \cdot R^3 \quad \text{(III)}$$

$$\text{Apparent viscosity} = \mu_a = \frac{\tau_a}{\gamma_a} \quad \text{(IV)}$$

where ΔP represents the pressure drop through the capillary, Q the volume flow through the capillary, and R and L the radious and length of the capillary, respectively.

Two corrections should be done on this approximation to obtain a more exact value of the viscosity: the Bagley correction and the Rabinowitsch correction. The Bagley correction takes into account the pressure losses at the entrance and end of the capillary and those should not be considered as a pressure drop in the capillary. This correction requires repeating the measuring test with capillary dies of different lengths. The Rabinowitsch correction is a correction to account for the non-Newtonian behavior if that is the case (most of the polymers).

1.4. Characterization techniques

1.4.1. Electrical properties

The electrical properties of the different materials were determined with a two-terminal sensing technique as done in the work by Henrik Oxfall [4]**.**

The technique involves the application of a voltage difference between the two ends of a specimen and measuring of the current through the sample. For that purpose two cables connected to the voltage source are clamped in series with the specimen. The specimen edges was coated with conducting silver paint in order to reduce the contact resistance between the specimens and the cables.

The current through the specimen was then measured with a multimeter in series with the voltage source. The volume resistance R is given by the Ohm's law as follows:

$$R = \frac{V}{I} \tag{V}$$

being V and I the voltage applied and current measured, respectively.

Once the specimen dimensions are known, the conductivity can be calculated as:

$$\sigma = \frac{l}{A \cdot R} \tag{VI}$$

where σ represents the conductivity, l the length of the specimen, A the cross-section of the specimen and R its resistivity.

The two-point technique has however some drawbacks since the impedance contribution of the wiring and contact resistance are neglected. A four-point technique overcomes these problems.

2. Experimental

2.1. Raw materials

The material studied was a nanocomposite consisting of EBA as the polymeric matrix and CB and GNP as the conductive fillers. The combination of CB and GNP fillers, denoted in this work as a hybrid system, consists of 80 wt % (weight- %) of GNP and 20 wt% of CB of the total filler content.

EBA, in form of pellets, was supplied by Borealis AB (Sweden). The copolymer was a crosslinkable grade containing 17 wt % of butyl acrylate comonomer. The density of the material was 0.925 g/cm^3.

The CB used was the medium–structured CB Ensaco 260G provided by Imerys Graphite & Carbon (Switzerland) with a particle size of 45 μm and a BET nitrogen surface area of 70 m2/ g. Ensaco 260G was produced with the commercial production process Tymcal MMM which gives nearly grit-free CB from partial oxidation of a high purity petrochemical feedstock. No water or additive is used during processing, and therefore very low sulphur content, low ash content and very low ionic contamination are achieved. The dispersibility of this type of CB in a matrix polymer is considered very good, with the absence of large and hard agglomerates. Other features of this grade are low water absorption and convenience for high shear applications. The density of the material was 1.8 g/ cm$^{3.}$ The product was delivered in powder form.

GNP was provided by XG sciences Inc. (Lansing, MI, USA), under the trade name xGnP®. The grade selected was Grade M with a particle diameter of 5 μm, an average thickness of approximately 6 - 8 nm and a typical surface area of 120-150 m^2/g. According to the manufacturer, the electrical conductivity of the particles parallel to the surface was 10^7 S/m whereas perpendicular to that was 10^2 S/m. The density of the material was approximately 2.2 g/cm^3.

2.2. Percolation curve determination

The limits of the percolation zone as well as the percolation threshold determined the filler contents of interest for study. The electrical conductivity of composites with different weight percentages of hybrid filler were then measured. In addition, the percolation curves for composites with each filler alone were also determined in order to confirm any synergistic effect. The procedure in these last cases was analogous to that used for the hybrid composite.

Compounding

The series of composites with different loadings were produced using in a Brabender mixing chamber with a capacity of 50 cm^3. The required quantities of EBA pellets together with powders of CB and/or GNP were mixed at 170°C during 10 minutes and 100 rpm. After compounding the materials were pelletized.

Sample preparation

Extrudates of 1 mm diameter were obtained with a capillary viscometer for subsequent electrical characterization. The equipment used for this purpose was a Ceast Rheoscope 1000 6742/00 (Ceast SpA, Pianezza, Italy) with a hardened steel capillary with a length /diameter (L/D) ratio of 10/1 [mm/mm]. The melt temperature was set at 170°C in order to ensure complete melting. The piston velocity was set to 2 mm/min (equivalent to a shear rate of 24.3 s^{-1}).

Conductivity measurements

The electrical conductivity of the extrudates was measured. The method used is described in section 3.3.4.

2.3. Methods

The experimental phase could be divided into three stages. The first stage comprised the compounding and characterization of the hybrid material with the total filler content selected from the percolation curve (Figure 17). Stages two and three covered experiments and measurement on composites containing lower and higher filler contents than that selected from percolation curve. In this case, the filler contents selected from the percolation curve were 5 volume percentage (vol%) (stage 1) and 3.5 vol% and 11 vol% the latter two regarded as lower and higher values, respectively.

The compounding of the hybrid materials was a two steps process. First, a masterbatch with each filler i.e. composites with high filler contents, were compounded with a twin screw extruder. Second, hybrid materials were compounded with different types of screws in a single screw extruder in order to study how the processing parameters affect the properties of the final composite material. In some cases, a third step in which the materials from the single screw extruder were pressed through the capillary viscometer was added. Figure 15 shows an overview of the processing done for the different materials in this work.

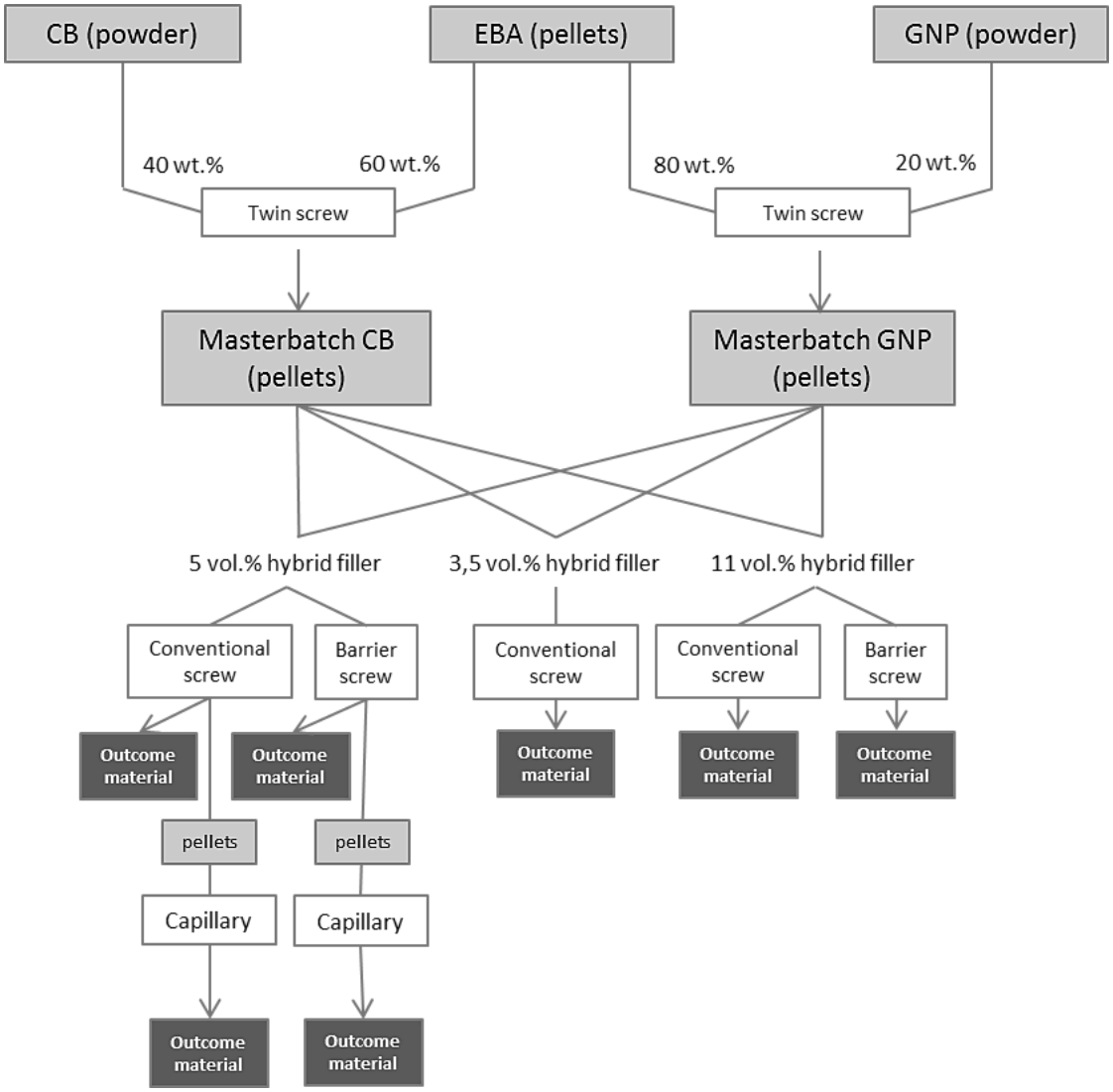

Figure 15. Overview of the processing done for the different materials

The characterization of the materials was performed with the following techniques

- Thermogravimetric analysis (TGA), for verification of filler content
- Conductivity test, for electrical properties determination
- Scanning electron microscope (SEM) and optical microscopy, for morphological characterization of fillers and hybrid material
- X-ray diffraction (XRD), for the structural analysis of GNP before and after compounding
- Uniaxial tensile test, for mechanical properties characterization
- Capillary viscometer, for viscosity determination

2.3.1. Compounding of masterbatches

As in the cable industry [44], masterbatches were used to carry the fillers. In this case, two masterbatches consisting of EBA with 20 and 40 wt % of GNP and CB, respectively, were compounded with a twin screw extruder. Table 2 shows the composition of both masterbatches**.** The content of filler in Masterbatch CB was chosen as the maximum content allowed, the viscosity being the limiting factor [45] whereas for the GNP masterbatch, it was the feeding difficulties and the possible interactions between platelets that could cause breakage of the same that determined the filler content.

Table 2 Composition of masterbatches

Description	Masterbatch
40 wt % of filler CB in EBA	Masterbatch CB
20 wt % of filler GNP in EBA	Masterbatch GNP

The equipment used for compounding was a Coperion (Stuttgart, Germany) ZSK 26 K 10.6 twin screw extruder with a configuration typically used to compound carbon black. Filler powders and EBA pellets were introduced through an electronic hopper, suitable for powders. The screw rotational speed was 230 rpm for the CB compounding and 120 rpm for the GNP. The rotation speed in the case of the GNP was determined in order to avoid GNP breakage. The temperature profile in the extruder from the hopper to the die was 150-170-170-170-170-170-170-170-170-175-175 °C.

The extruded strings were pelletized after compounding and TGA studies were performed in order to confirm the total filler content of the masterbatches.

A characterization of the GNP was performed with the SEM and the XRD technique before and after processing in order to study the effect of the twin screw extrusion on GNP. The effect of extrusion on CB was not analyzed, considering it as a dispersion of the aggregates in the matrix [46].

2.3.2. Extrusion experiments

Extrusion mixing was used to obtain composite materials with 3.5, 5 and 11 vol% total filler contents. In order to attain the different compositions, pellets from Masterbatch CB, Master Batch GNP and EBA were manually mixed in the corresponding weight percentages. Table 3 shows weight percentages of the base components (masterbatches and EBA) in the different composite materials.

Table 3. Weight percentages of masterbatches and EBA in composite materials

Description	Wt % Masterbatch CB	Wt % Masterbatch GNP	Wt %EBA
5 vol% hybrid filler content	5.35	42.81	51.84
3.5 vol% hybrid filler content	3.81	30.52	65.67
11 vol% hybrid filler content	10.98	87.85	1.17

The single screw extruder used was a Brabender compact extruder, Brabender OHG (Duisburg, Germany), with a screw diameter D of 19 mm and a screw length of 25D (25 times the screw diameter), three individually controlled temperature zones and a temperature controlled circular die with a diameter of 3 mm. A water bath system was used for cooling the extrudates.

5 vol% content of hybrid filler

For the composites with 5 vol% filler content, a total of 16 experiments were carried out combining the following variables:

1. Two types of screw: barrier-flightened screw and conventional screw. The barrier-flighted screw (Maillefer, 1960;1967) had a compression ratio of 2:5:1 and a Saxton distributive mixing element. The conventional screw had a compression ratio of 1:2
2. Two screw speeds: 50 rpm and 100 rpm
3. Two temperature profiles in the extruder and die zones: 90/140/160/160°C and 90/140/180/180°C.

From the extrudates, some strings (with a length of 20 cm) were produced with a capillary viscometer. The equipment and processing conditions are analogous to those described in section 3.2.

Table 4. Lists all the experiments performed with the composite containing 5 vol% of hybrid filler

Table 4. Experiments performed with the composite containing 5 vol% of hybrid filler.

Experiment	Processing				Notation
	Screw	Screw speed (rpm)	Temperature profile (°C)	Capillary viscometer	
1	Conventional	50	90/140/160/160	No	160C50-5%
2	Conventional	50	90/140/180/180	No	180C50-5%
3	Conventional	100	90/140/160/160	No	160C100-5%
4	Conventional	100	90/140/180/180	No	180C100-5%
5	Conventional	50	90/140/160/160	Yes	160C50-5% Cap
6	Conventional	50	90/140/180/180	Yes	180C50-5% Cap
7	Conventional	100	90/140/160/160	Yes	160C100-5% Cap
8	Conventional	100	90/140/180/180	Yes	180C100-5% Cap
9	Barrier	50	90/140/160/160	No	160B50-5%
10	Barrier	50	90/140/180/180	No	180B50-5%
11	Barrier	100	90/140/160/160	No	160B100-5%

12	Barrier	100	90/140/180/180	No	180B100-5%
13	Barrier	50	90/140/160/160	Yes	160B50-5% Cap
14	Barrier	50	90/140/180/180	Yes	180B50-5% Cap
15	Barrier	100	90/140/160/160	Yes	160B100-5% Cap
16	Barrier	100	90/140/180/180	Yes	180B100-5% Cap

3.5 vol% content of hybrid filler

In the case of the composites with 3.5 vol% of filler content, the number of experiments were reduced to those corresponding to the best outcomes found in the case of 5 vol% total filler content. The screw used in this case was the conventional one and the operation conditions were a temperature profile of 90/140/160/160°C and a screw speed of 50 rpm.

Table 5. lists the experiment performed with the composite containing 3.5 vol% of hybrid filler

Table 5. Experiments performed with the composite containing 3.5 vol% of hybrid filler

Experiment	Processing				Notation
	Screw	Screw speed (rpm)	Temperature profile (°C)	Capillary viscometer	
1	Conventional	50	90/140/160/160	No	160C50-3.5%

11 vol% content of hybrid filler

The composite with the higher filler content (11 vol%) was produced in order to study the plateau behaviour clearly above the percolation threshold . Two experiments were carried out; the temperature profile and screw speed were in both cases 90/140/160/160°C and 50 rpm, respectively. In this case, both types of screws were used.

Table 6. lists the experiments performed with the composite containing 11 vol% of hybrid filler

Table 6. Experiments performed with the composite containing 11 vol% of hybrid filler

Experiment	Processing				Notation
	Screw	Screw speed (rpm)	Temperature profile (°C)	Capillary Viscometer	
1	Conventional	50	90/140/160/160	No	160C50-11%
2	Barrier	50	90/140/160/160	No	160B50-11%

2.3.3. Verification of filler content (TGA)

TGA was run on the extrudates in order to verify the amount of filler added. The verification was performed on the compounded masterbatches, and also, on the extruded hybrid composites.

The equipment used was TGA/DSC 1 Star system, Mettler Toledo, from Switzerland with a sensor type K. A total of 3 different measurements were done for each specimen.

2.3.4. Electrical measurements (two-point measuring technique)

Conductivity tests were performed in order to determine the effect on the electrical properties of the differently processed materials. For this purpose, 15 string specimens with a length of 25 mm from the differently processed samples were used (tables 4, 5 and 6). The same method was also employed for determining the percolation curve. The diameters of the specimen varied according to the manufacturing process, see Table 7.

Table 7. Diameters of the differently processed specimens

Manufacturing process	Specimen diameter
Capillary	1 mm
Extrusion	2,5-3 mm

Sample preparation

The specimens were prepared by cryofracturing the selected strings. The conductive fillers should to be present at the two fractured surfaces of the specimens, which is obtained in brittle fracture. For this purpose, strings with similar diameters were held between two rectangular steel plates with dimensions 25 X 70 mm. Two shallow surface incisions were made in order to facilitate the fracture at the desired points. The support with the strings was immersed in liquid nitrogen (1 min for the strings with 1 mm diameter and 2 minutes for the others) in order to enable brittle fracture. The final dimensions of each specimen were measured with a digital caliper with a resolution of 0.01mm and accuracy of 0.03mm. Conductive silver paint was applied at the two ends of the specimens. Before testing, the specimens were dried in a fume box for 24 hours in order to allow the paint to dry and ensure sufficient adhesion to the composite.

Measurements

Two-point conductivity measurements were performed to measure the electrical conductivity according to the ASTM D257-07 standard test method. The equipment used, shown in Figure 16, used a system power supply Sorensen DCS300-3.5E DC from Ametek (United States of America) placed in an insulating box. A digital multimeter Fluke 846A was used for measuring the direct current through the specimens.

The specimens were fixed between the clamps and the tests performed in an isolating box prepared for this purpose. The criteria followed when performing the measurements is shown in Table 8. Low voltages were applied to specimens with high electrical conductivity whereas high voltages were applied to those with low conductivity values.

Table 8. Voltages applied to specimens according to their conductivities

Conductivity	Applied voltage
Above 10^{-3}S/cm	10V
Between 10^{-3} and 10^{-5}S/cm	100V
Below 10^{-5}S/cm	300V

Since the specimen conductivities were unknown, a low voltage was initially applied and then gradually increased until the conductivity started to decrease. This method is known as the CABOT method. The conductivity was determined using equation (V) and (VI) as described in section 2.4.1

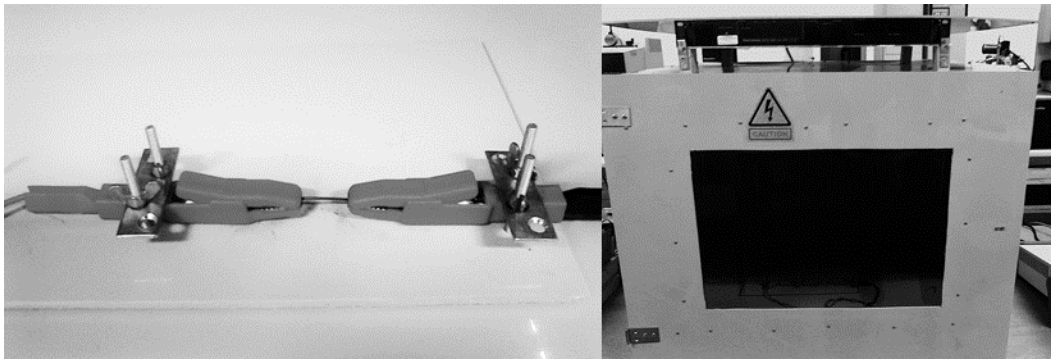

Figure 16. Two-point measuring technique used for electrical measurements

2.3.5. Morphological characterization of composite material and fillers (SEM and Optical Microscopy)

SEM

Information on the shape, size and orientation of the fillers before and after compounding and of the composite materials was obtained by means of a digital scanning electron microscope Carl Zeiss DSM 940, Oberkochen, Germany. The composite samples containing the thermoplastic polymer were coated with an approximately 5 nm thick gold layer using a Sputter Coater S150B, BOC Edwards, UK.

Sample preparation

Different samples preparations were required for the different materials studied. When analyzing the filler after compounding, the polymer matrix was removed. Pellets of the compounded materials were heated from 20 to 600°C at 10 °C /min in an argon atmosphere in a tube furnace Entech. When analyzing the microstructure of the composite, the cross-sections obtained by cryofracturing the strings were used.

Optical microscopy

Samples of the compounded materials were also observed in an optical microscope in order to study the orientation and distribution of the platelets. The equipment used for that purpose was a Leitz DMXR optical microscope, Germany. The studied samples were taken from the extruded strings and mounted with the cold mounting technique in order to examine a cross section. They were grinded with 120 grit paper and polished with 9, 3 and 1 μm diamond paste. The polished surfaces were directly observed with magnifications of 200 and 500 times and analyzed with the software AxioVision (AxioVs40, version 4.9.1.0). Analyses of areas, length, widths of the platelets and distances between them were performed.

2.3.6. Structural analysis of GNP (XRD)

In order to assess a possible exfoliation of the GNPs, XRD was applied to fillers and pellets of the composite material Powders of pristine GNP and CB, GNP after compounding the masterbatch and hybrid filler after compounding with the single screw extruder were studied. When required, the polymer matrix was removed by thermal decomposition in a furnace, as done for the SEM sample preparation. The incentive for this last study was the possible intercalation of the polymer between the graphite nanoplatelets.

The equipment used was a Bruker D8 Advance X-Ray diffractometer. The radiation source was CrKα with a wavelength of 2.2897 Å. The generator was set to 35kV and 40 mA. Spectra were recorded every 0.02° with steps of one second.

2.3.7. Uniaxial tensile tests

Uniaxial tensile test were performed on the extruded strings. For that purpose, strings 80 cm long from extruded EBA and composites containing 3.5 and 11 vol% of hybrid filler extruded with both the conventional and the barrier screw were used. Here, the mechanical tests were performed at the same conditions used in previous work [47] in order to compare the results.

The equipment used was a hydraulic tensile tester, Zwick Z2.5 Tensile testing machine, equipped with a load cell of 500N (manufactured by A. S. T. GmbH Dresden). The clamps used were specific for testing string specimens. The strings were rolled around the clamps leaving a gauge length of 70 mm. Twelve specimens of each material were tested at room temperature, using a speed of 70 mm/min order to reach a deformation rate of 100 %/min. A preload of 1.2 N was applied in all the tests.

2.3.8. Rheological measurements (Capillary Viscometer)

Rheological measurements were performed in order to assess the influence of the filler particles on the melt viscosity. The equipment used was a Gottfert Rheograph 2002 Germany capillary viscometer. The polymeric matrix as well as composites containing 3.5 and 11 vol% of filler content were used.

4. Results and discussion

4.1. Percolation threshold

Figure 17 shows the percolation curve of the hybrid filled polymer studied in this work. As can be observed, the slope of the curve became steeper in the range 2-4 vol% filler and the conductivity was levelled out around 14 vol%, reaching a value of 0,065 S/cm at 14 vol%. A main percolation threshold value at around 3 vol% could be established and a second less pronounced at approximately 7 vol%.

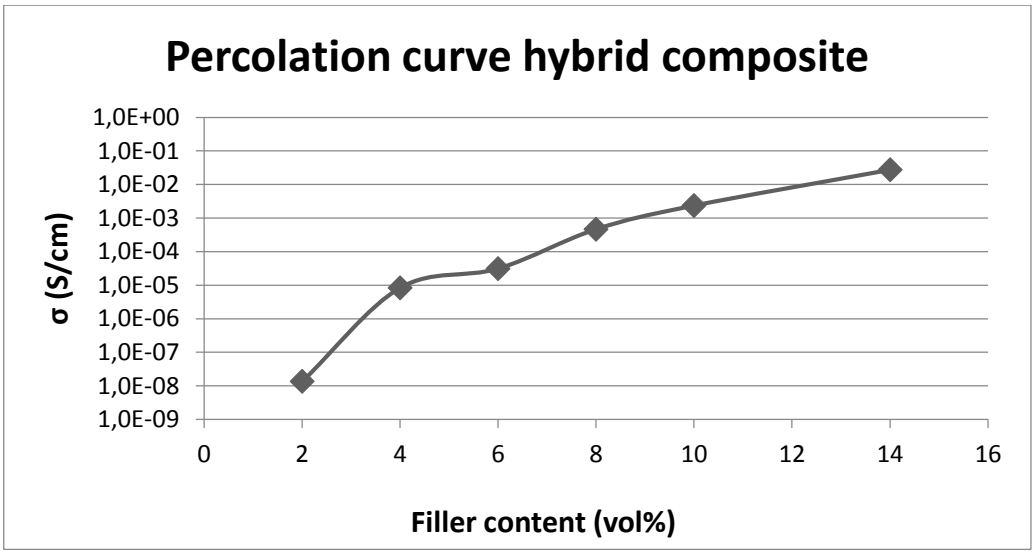

Figure 17. Percolation curve for EBA filled with the hybrid system GNP/CB 80-20 compounded with the internal mixer.

As perhaps expected, the percolation zone in the hybrid filled system was achieved at lower filler contents than the systems filled only with GNP or CB, showing the synergistic effect on the electrical properties when GNP and CB are combined as a filler, Figure 18.

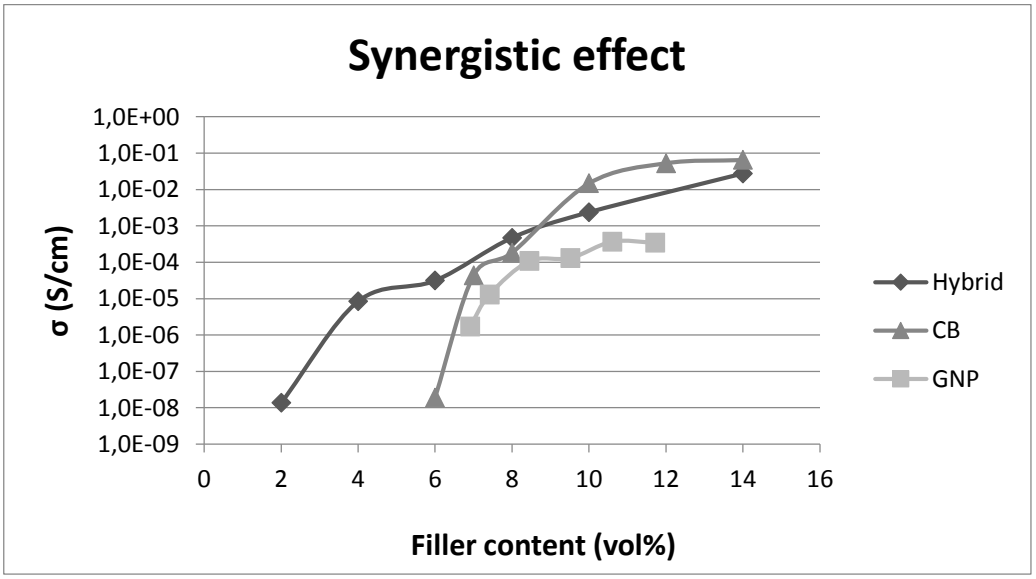

Figure 18. Synergistic effect between CB and GNP fillers on the electrical properties of filled EBA. The three filled systems were compounded with the internal mixer.

As suggested in ref [4], the synergistic effect could be a consequence of the insertion of CB between GNP particles (due to geometrical and size differences) thus linking as a result the GNP particles together even at low CB additions (20 weight unit per each 80 units of GNP).

In order to study the effect of processing on the hybrid filled system, the volume percentages of interest were set to 3.5, 5 and 11 wt %.

4.2. Electrical conductivity

The results from the conductivity measurements of the differently processed materials with 5 vol% filler are shown in Figures 19 and 20. The values shown are the average values of a total of 15 measurements and the standard deviations are given in Tables 9 and 10. In all cases, the reference values were obtained from the percolation threshold curve, i.e. materials compounded in the mixing chamber and forced through the capillary viscometer. The data presented in Figure 19 correspond to the materials extruded with the conventional screw, whereas Figure 20 shows the results in the case of the barrier flighted screw.

It could be observed that the conductivities obtained with the conventional screw overcome in some cases that of the reference material with 3 orders of magnitude whereas the conductivities obtained with the barrier screw were 3 or 4 orders of magnitude lower than that of the reference material. It could be concluded that the conventional screw led to a more efficient microstructure in terms of dispersion of the fillers in the matrix than both the barrier screw and the mixing chamber. For the particular case of the composites that had passed through the capillary viscometer after extrusion mixing (indicated as Cap in the sample name), the opposite trend was observed. The conductivity of the material obtained with the conventional screw decreased whereas for the material processed with the barrier screw it increased. This could be due to a reorientation effect caused by the capillary, or a possible accumulation effect of filler in the central region of the samples. The first effect can be considered as negative for the electrical properties of the filled systems due to the loss of possible contacts between platelets. The second effect could possibly contribute positively to the electrical properties of the materials compounded with the barrier screw.

Regarding the influence of the processing temperature and the screw speed on the conductivity, no major differences were observed. Therefore the changes in shear stresses due to lower temperature or higher rotational speeds are assumed to be small within the ranges of temperatures and rotational speeds used here.

Table 9 Average values of conductivities and standard deviations for 5 vol% hybrid filled systems processed with the conventional extruder

Sample	Conductivity average (S/cm)	Standard deviation
160C50 5% Cap	4.5E-04	1.96E-04
160C100 5% Cap	1.5E-04	1.67E-04
180C50 5% Cap	7.5E-04	6.10E-04
180C100 5% Cap	6.6E-04	7.86E-04
160C50 5%	1.4E-02	5.96E-03
160C100 5%	6.1E-03	3.72E-03
180C50 5%	3,6E-03	2.06E-03
180C100 5%	7.3E-03	4.86E-03

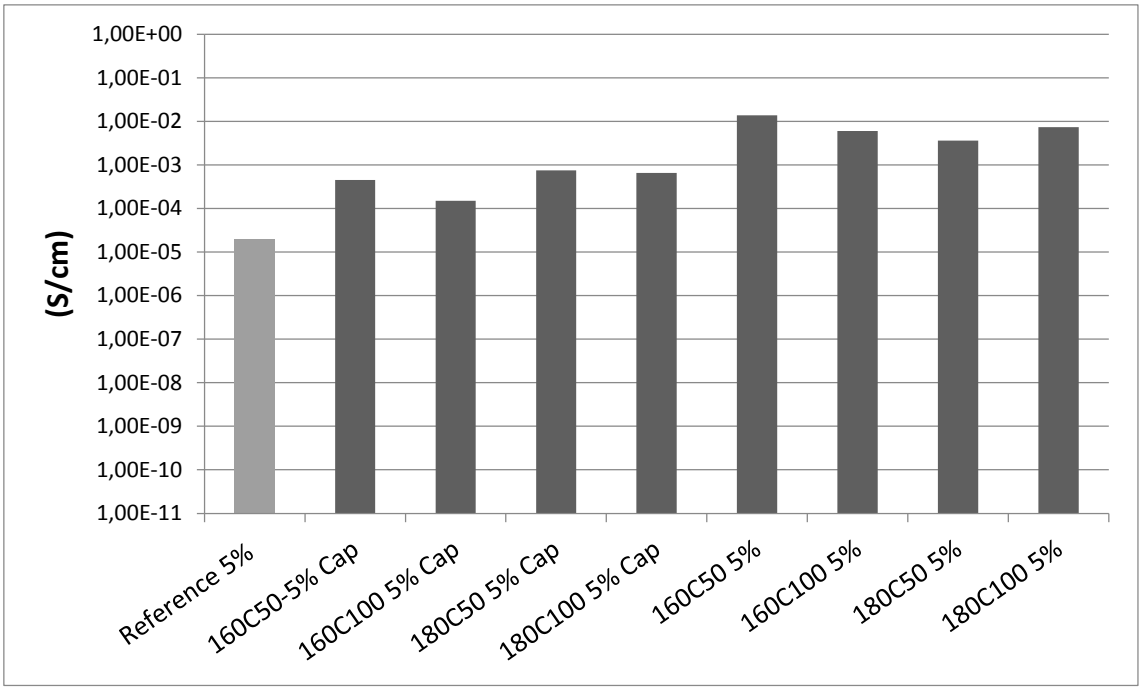

Figure 19. Electrical conductivities of 5 vol% hybrid filled systems processed with the conventional screw and a comparison with secondly processed materials in a capillary viscometer. The first bar shows the reference conductivity from the percolation curve.

Table 10. Average values of conductivities and standard deviations in 5 vol% hybrid filled systems processed with the barrier extruder

Sample	Conductivity average (S/cm)	Standard deviation
160B50-5% Cap	7.1E-09	3.96E-10
160B100 5% Cap	7.6E-09	3.56E-10
180B50 5% Cap	7.7E-09	3.64E-10
180B100 5% Cap	8.3E-09	6.60E-10
160B50 5%	8.6E-10	5.82E-11
160B100 5%	7.9E-10	1.52E-10
180B50 5%	9.7E-10	4.55E-11
180B100 5%	8.3E-10	1.63E-10

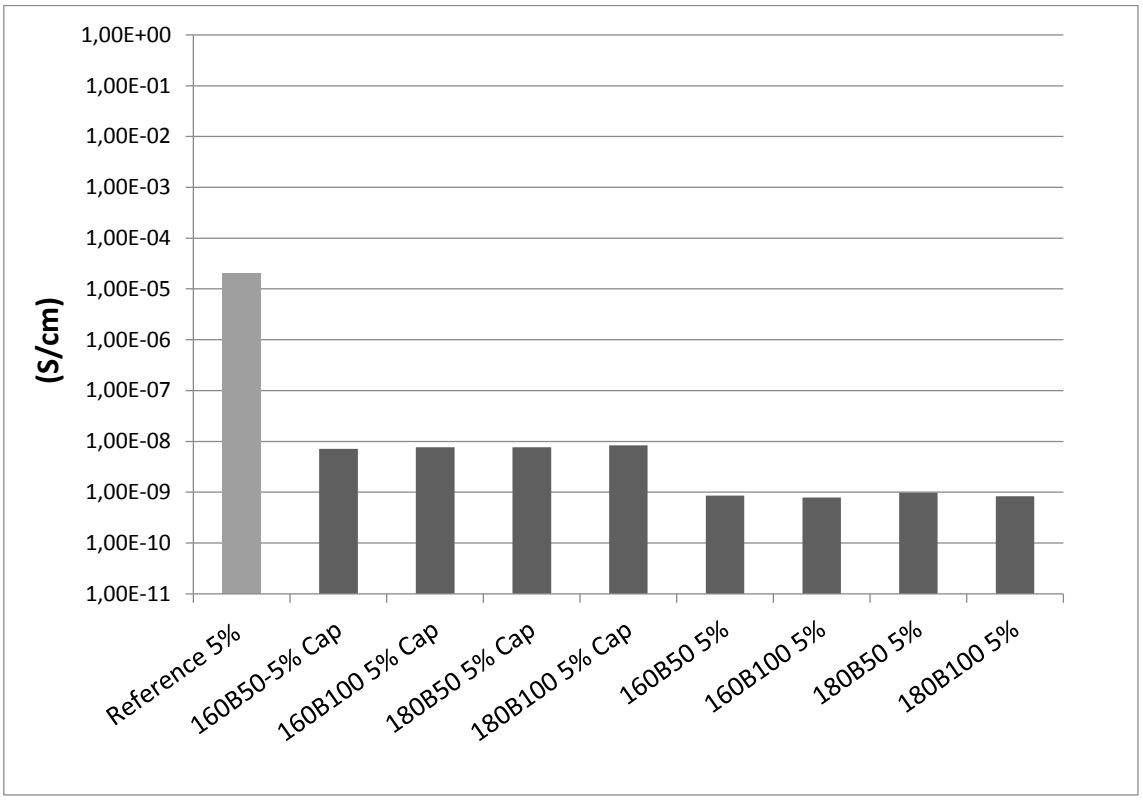

Figure 20 Electrical conductivities of 5 vol% hybrid filled systems processed with the barrier screw and a comparison with secondly processed materials in a capillary viscometer. The first bar shows the reference conductivity from the percolation curve

The effect of processing on the electrical properties for materials with different filler contents and compounded with both screws at 160 °C and 50 rpm is shown in Figure 21. Comparing the conductivities obtained with those from the percolation curve in Figure 17, it could be seen that the conductivity increased in three orders of magnitude for the 3.5 vol% filled system whereas for the 11 vol% filled system, the increase was smaller than one order of magnitude. The results from the 3.5 vol%, 5 vol% and 11 vol% of filler content described a percolation curve where the conductivity seemed to be established below 5 vol% content, reaching a similar value to the one reached with the highest filler contents in Figure 17. As a conclusion, the beneficial microstructure obtained with the conventional screw process appeared to be present at as low filler contents as 3.5 vol% and the conductivity levelled out at 11 vol%.

The last two bars in Figure 21 indicate the conductivity of 5 and 11 vol% hybrid filled systems processed with the barrier screw. The screw speed and die temperature were again 50 rpm and 160°C respectively. Comparing the conductivities of the materials containing 5 vol% and 11 vol% and extruded with the barrier screw with the conductivities obtained with those from the percolation curve in Figure 17, it could be seen that the conductivity decreased in three orders of magnitude at 11 vol%. This drop in conductivity could be due to the destruction of the network caused by the efficiency of the barrier screw in dispersing the particles.

Table 11. Average values of conductivities and standard deviations for systems with different hybrid filler contents processed with the conventional and barrier screws

Sample	Conductivity Average (S/cm)	Standard deviation
160C50 3.5%	1.8E-03	1.10E-03
160C50 5%	1.4E-02	5.96E-03
160C50 11%	1.3E-02	2.73E-03
160B50 5%	8.6E-10	5.82E-11
160B50 11%	1.8E-05	1.81E-06

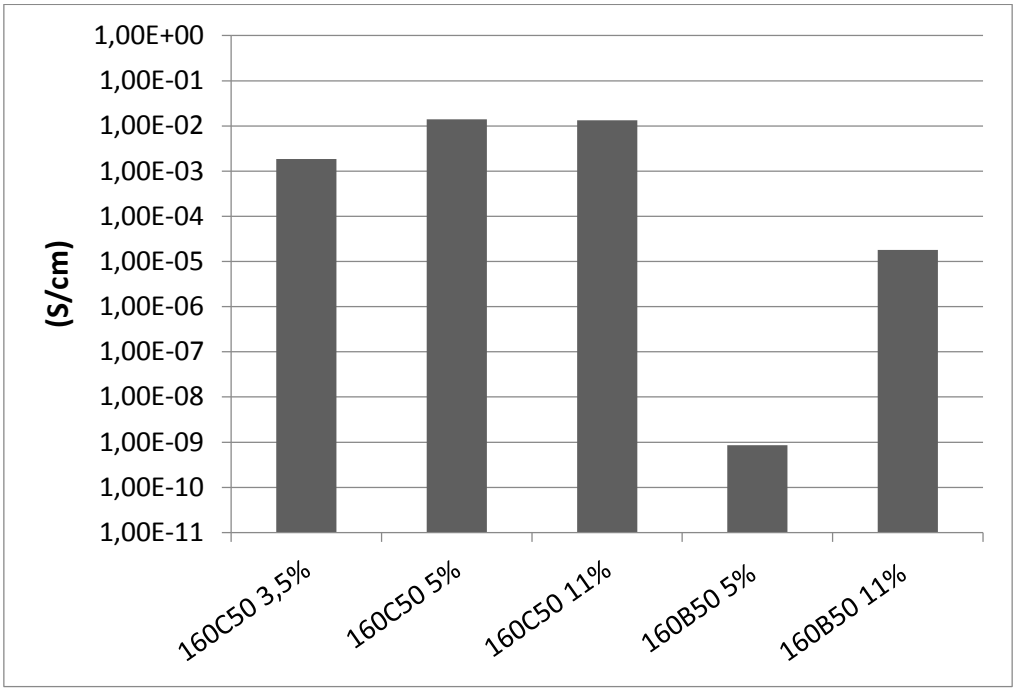

Figure 21. Electrical conductivities of systems with different hybrid filler contents processed with the conventional and barrier screws. The three first bars show the conductivities of samples processed with the conventional screw whereas the last two bars show those processed with the barrier screw. All samples were extruded at a screw speed of 50 rpm of screw rotation speed and a temperature in the die of 160°C.

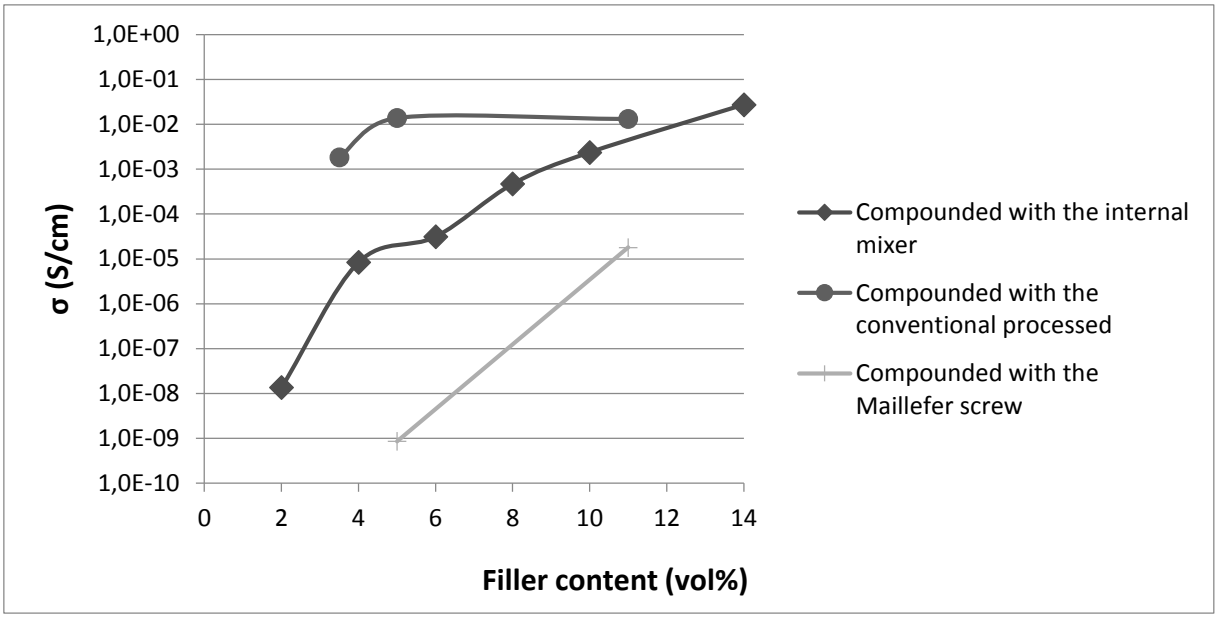

Figure 22 Comparison of conductivities of materials processed with the conventional and barrier screws to these of the reference material compounded with the internal mixer.

4.3. Morphological study of fillers

The microscopical examination of the GNP filler before and after the twin-screw extrusion used for the masterbatch compounding revealed a low degree of breakage of the platelets. Many platelets with the pristine size (5 μm diameter) could be observed after the processing. Figure 23 (left) shows the GNP after compounding with the twin screw.

Furthermore, the pictures taken with SEM of the filler particles after processing with the conventional and the barrier screw also showed the presence of platelets with the original size. Figure 23 (right) shows the GNP after compounding with the barrier screw. However, due to the difficulty determining the degree of breakage in these images, a comparison between the two compounding techniques was not possible to make. More accurate results were expected from the microstructural analysis on the composite material.

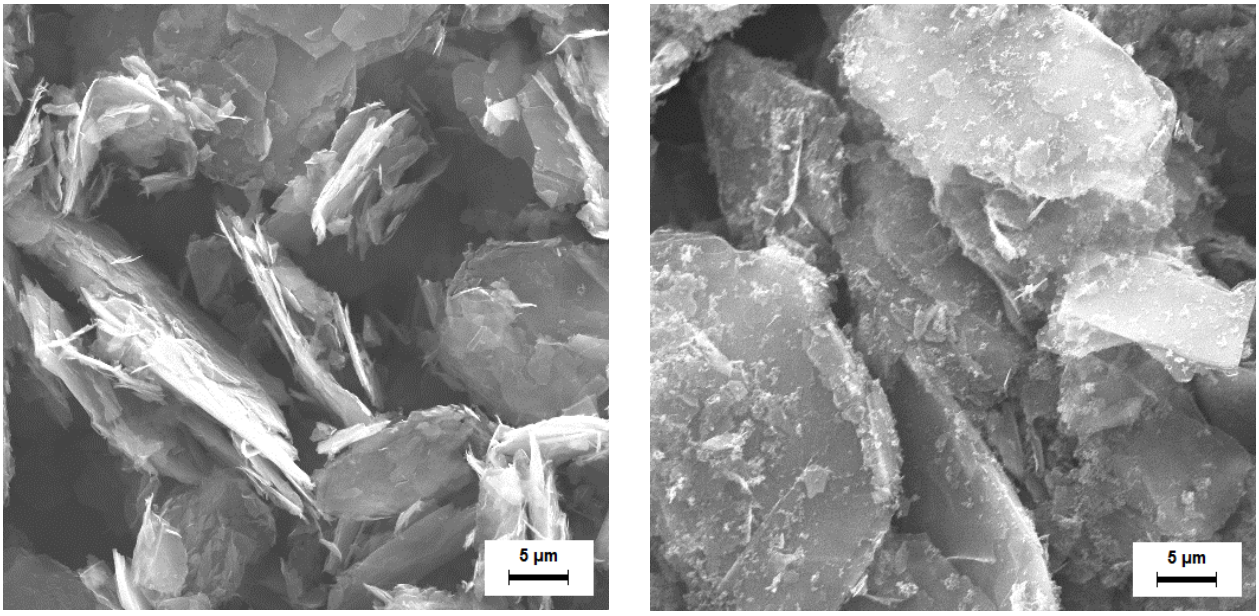

Figure 22. SEM pictures of the GNP after compounding the masterbatch with the twin screw extruder (left) and filler (GNP and CB) after extrusion with the barrier screw (right)

4.4. Morphological study of filled polymer

Figures 24 and 25 show the microstructure of the filled polymer systems processed with the conventional and the barrier screw at an 11 vol% filler content, respectively. The micrographs, taken with the optical microscope, reveal a total area of 0.5 mm^2 of the total 7.06 mm^2 of the cross-section of the extrudates. The photos were taken from similar zones in both extrudates from the points indicated in the appendix A. A tendency of the GNP agglomerates to be placed in the peripheral region of the extrudate was observed. A higher degree of orientation was also noted in the peripheral region than in the central region even though the degree of orientation was not high in any case. A significant amount of voids was present in both processed materials.

When comparing the material with higher conductivity (Figure 24, processed with the conventional screw) with that of lower conductivity (Figure 25, processed with barrier screw), longer platelets were observed in the first case. In addition, a tendency for two agglomerates to be very close to each other was observed in the case of the specimen with higher conductivity.

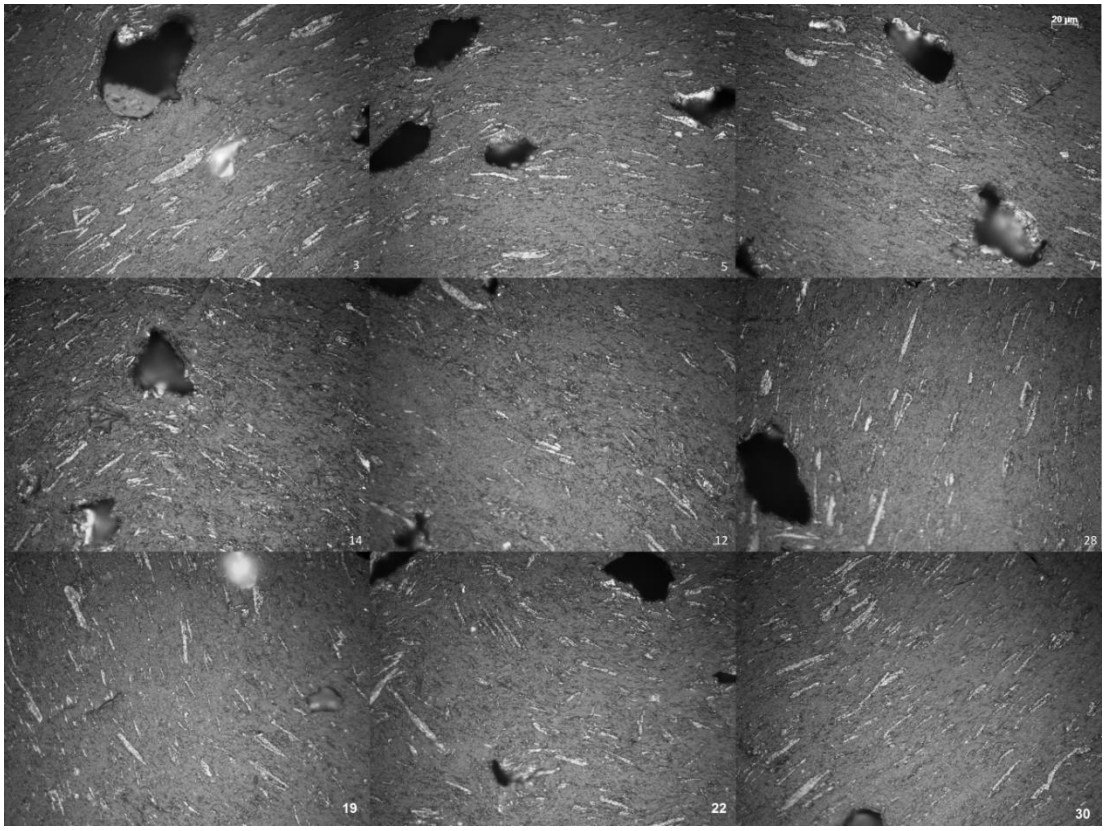

Figure 23 Optical micrograph of a cross-section from sample extruded with the conventional screw at 50 rpm and 160°C at the die with 11vol% filler content. 500 times magnification

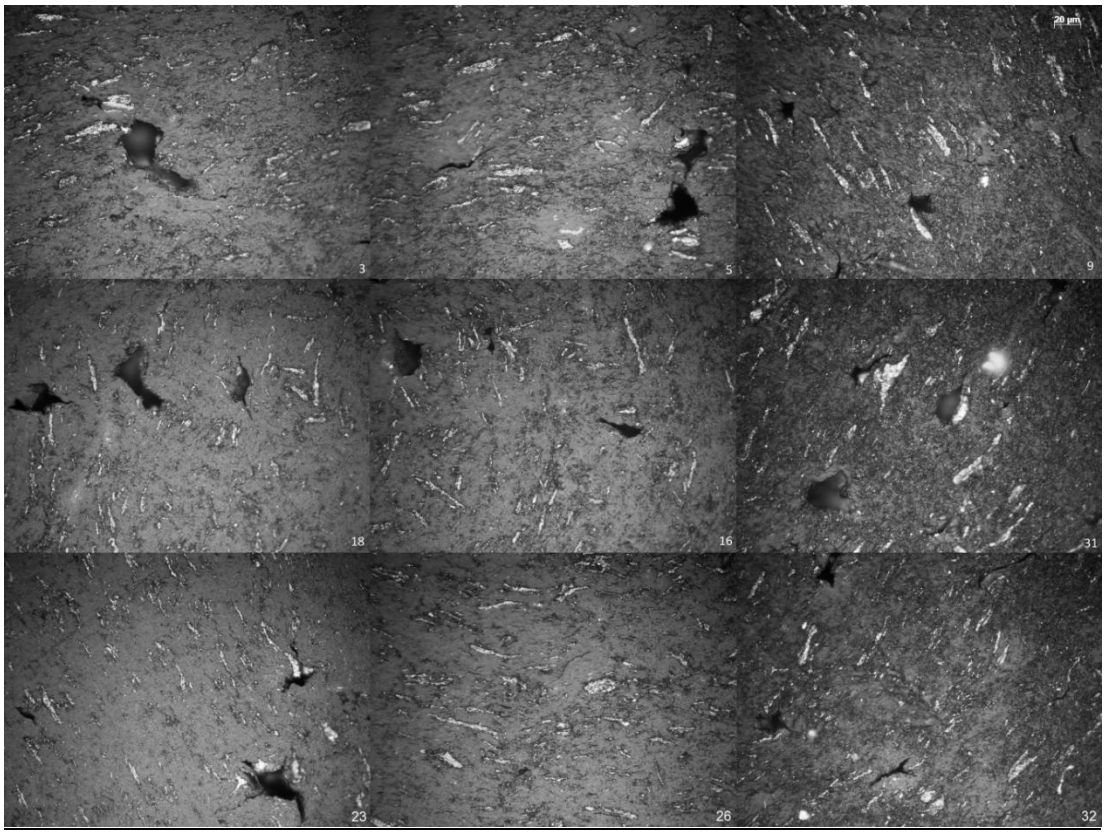

Figure 24. Optical micrographs of a cross-section from sample extruded with the barrier screw at 50 rpm and 160°C of temperature at the die with 11vol% filler content. 500 times magnification.

These observations were supported by the image analysis of the areas, lengths, widths and distances between platelets obtained with the software AxioVision as shown in appendix A. The measured lengths were taken from platelets longer than 10 µm. The analysis performed on the photos in Figures 24 and 25 is summarized in Figure 26. Larger amounts of platelets with longer lengths were observed when using the conventional screw than in the samples extruded with the barrier screw. These results together with the analysis of areas shown in Figure 27 indicated that not only the number of longer platelets was larger in the materials processed with the conventional screw but in general the number of platelets of any length was larger in the case of the conventional screw. An excessive breakage could therefore be the reason for the negative effect of the barrier screw on the electrical properties of the filled polymer. This hypothesis was supported by the assumption that particles with a higher aspect ratio enhanced the formation of conductive networks [27].

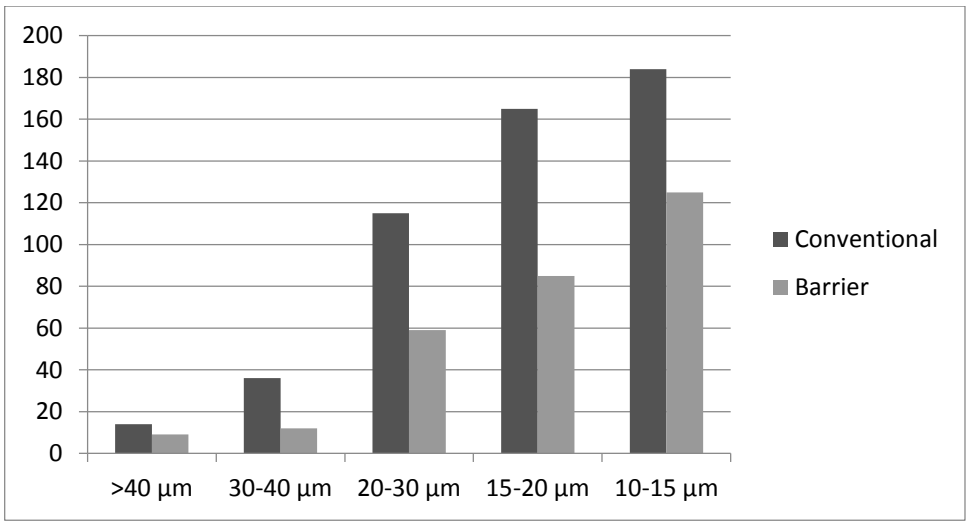

Figure 25. Comparison of the lengths of platelets in samples processed with the conventional and the barrier screw. Analysis made on photos shown in Figures 24 and 25

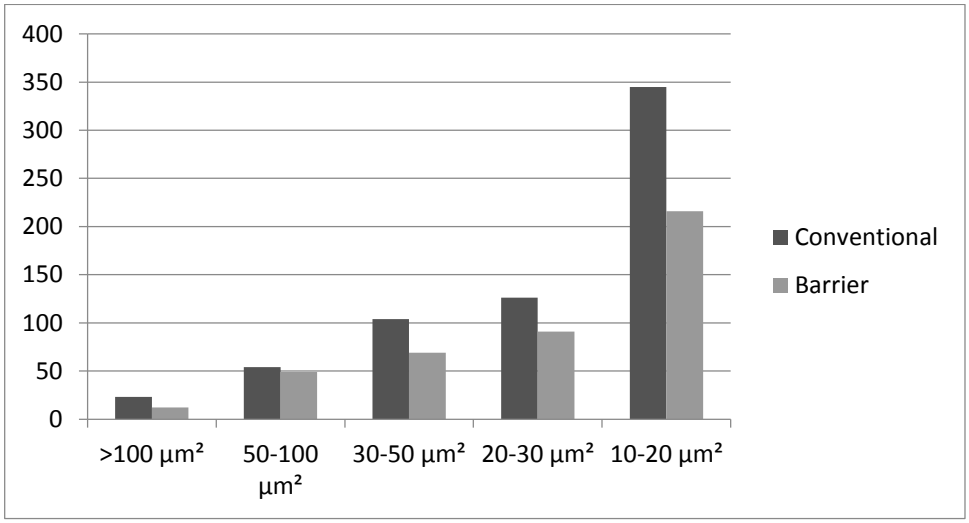

Figure 26. Comparison of the areas of the platelets in samples processed with the conventional and the barrier screw. Analysis made on photos shown in Figures 23 and 24

The widths analysis of the platelets is shown in Figure 28. The measured widths were taken from platelets with thicknesses greater than 1.5 µm. In this case, no significant differences were detected between the differently processed materials.

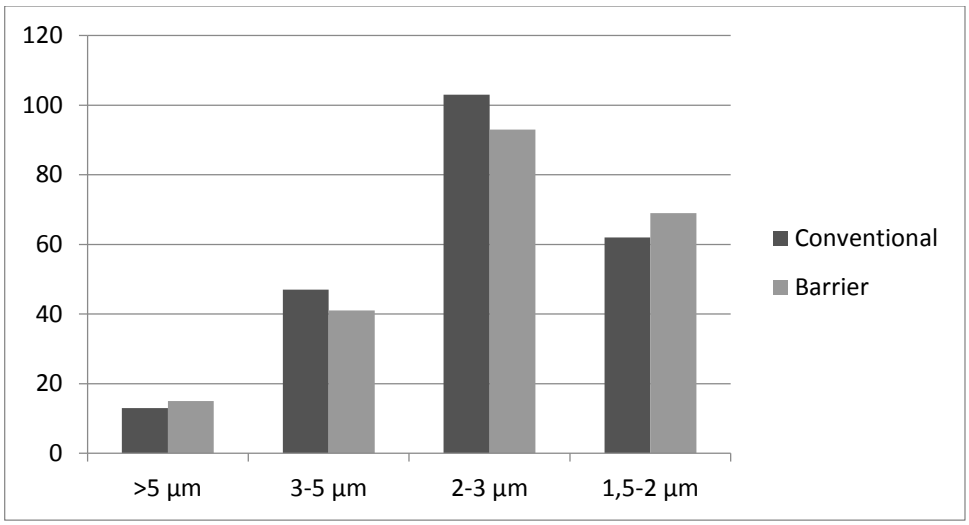

Figure 27. Comparison of the widths of platelets in samples processed with the conventional and the barrier screw. Analysis made on samples with 11 vol% filler content extruded at 50 rpm and with a temperature in die of 160°C.

The results from the analysis of distances between platelets is shown in Figure 29. The measured distances were taken from platelets separated less than 4 µm since the interest was focused on closely separated platelets. In specimens produced with the conventional screw, the particles tended to be closer together.

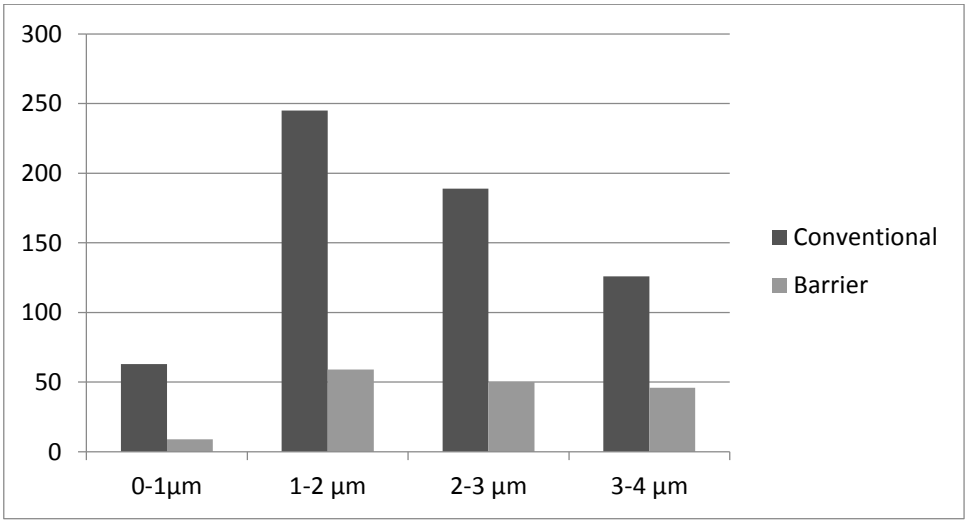

Figure 28. Comparison in distances between platelets in samples processed with conventional and barrier screw. Analysis made on samples with 11 vol% filler content extruded at 50 rpm and with a temperature in die of 160ºC.

The results from the image analysis of the materials extruded with the barrier screw were consistent with the speculations regarding network destruction from the conductivity measurements. The presence of visually detectable platelets was low and therefore a reduction of the platelets to very small sizes was suspected.

In the case of the conventional screw, the effective microstructure indicated from the conductivity results, was supported by the results of a relatively large amount of not-broken platelets with a close distance between them. Although it could not be quantitatively measured, some exfoliation of the platelets in the thickness direction could be speculated on. The presence of two thin platelets close to each was observed in the optical micrographs. This could explain the sharp increase in conductivity with increasing filler content with the conventional screw compared to the reference materials processed with the internal mixer since previous studies showed no major differences in the orientation or distribution of particles and a breakage of the platelets was neither expected [31]. However, regarding the exfoliation of the platelets, no definite conclusion could be drawn and further studies are needed.

Further studies of the microstructure were made with the SEM, Figure 30. Indications of pulled-out particles are clearly revealed which points to a rather poor adhesion between the filler and the matrix material.

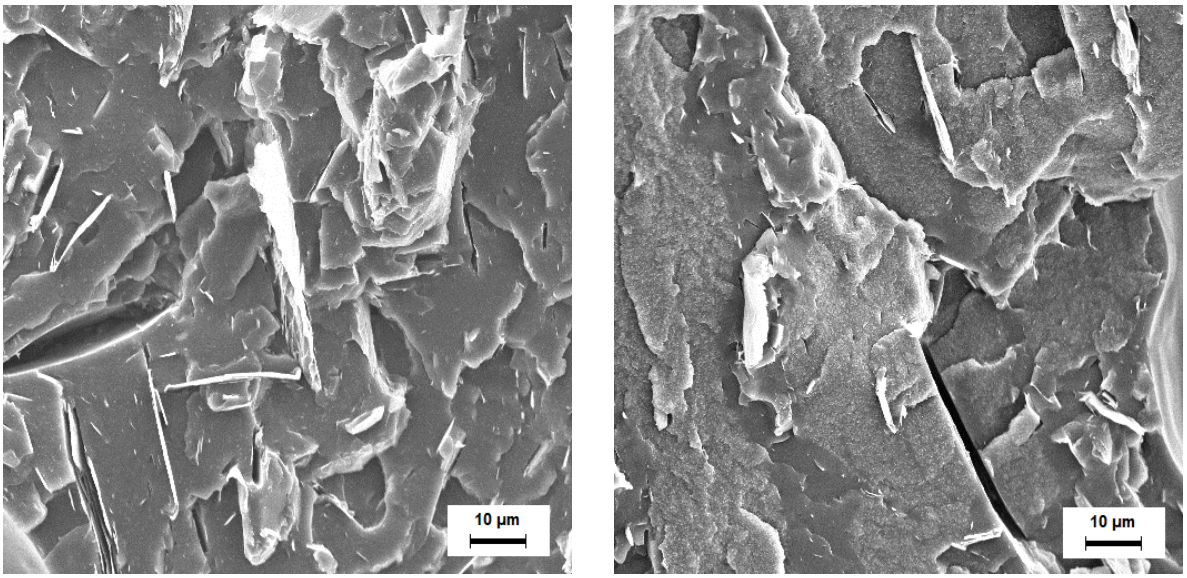

Figure 29. Scanning electron micrographs of fractured surfaces of samples extruded with the barrier screw (left) and the conventional screw (right).

4.5. Structure of GNP as revealed by XRD

The structural results from the XRD analysis are shown in Figures 31 and 32. Figure 31 is a comparison of the diffractograms of the pristine GNP powder, the fillers extracted from the polymer after different processing histories and the filled polymer extruded with conventional screw at 50 rpm and 160 °C for 5 vol % of filler content. The same position of the peaks mostly corresponding to graphite was observed in all the samples processed with different temperatures and rotation speeds and the pristine filler. The position of the peaks for the sample with the polymeric matrix also coincided with these, showing an additional peak corresponding to the crystalline regions of the polymer as seen in Figure 32.

Peaks at 39.8°, 64.96°, 68.59°, 86.06° and 136.92° correspond to the crystallographic distances between the planes (002), (100), (101), (004) and (110), respectively. The presence of other detected planes was attributed to impurities present in the GNP filler since they were present in the pristine grade. The distances between the (002) planes and between the (004) planes provide the same information, giving the basal plane distance or distance between graphene layers. The determined basal plane distance was 0.336 nm, very similar to the corresponding one for graphite (0.335 nm) indicating no separation of the graphene planes. The intensity and broadness of these peaks could relate to the agglomeration of the graphene layer in the platelets and therefore a possible exfoliation of these. Planes (100) and (110) correspond to those perpendiculars to the graphene layers. Therefore the intensity and broadness of these peaks could be related to the diameter of the platelets. [48]

From the comparison of the shapes and positions of the peaks no significant differences were observed between the pristine and processed fillers and neither between the processed materials with the different screw speeds, processing temperatures or screw type. In the case of the pellet, the intensities were substantially reduced, the reason being the lower amount of platelets due to the presence of the polymeric matrix and the lower degree of orientation of the platelets in the sample holder.

However, the magnitude of the intensity and the broadness were not considered to be reliable since these depend on the orientation of the platelet in the sample holder and the particles in the form of powder could be affected during the sample preparation. Therefore a more reliable analysis of the intensity of the peaks was expected from the study of the platelets in the pellets.

Figure 32 shows the comparison between the diffractograms of the EBA pellets, pellets from the GNP masterbatch and the processed pellets with the barrier and conventional screws (50 rpm, 160 °C and 5 vol% of filler). No significant differences could be observed in the peaks shapes or positions between the materials processed with the barrier and the conventional screw. Therefore no conclusions could be drawn about the separation of the graphene planes, possible exfoliation of these or the platelet diameter sizes. When compared to the masterbatch diffratogram a higher intensity of the peaks is seen for this material, the reason being the higher concentration of platelets in the masterbatch (20 vol% of GNP content).

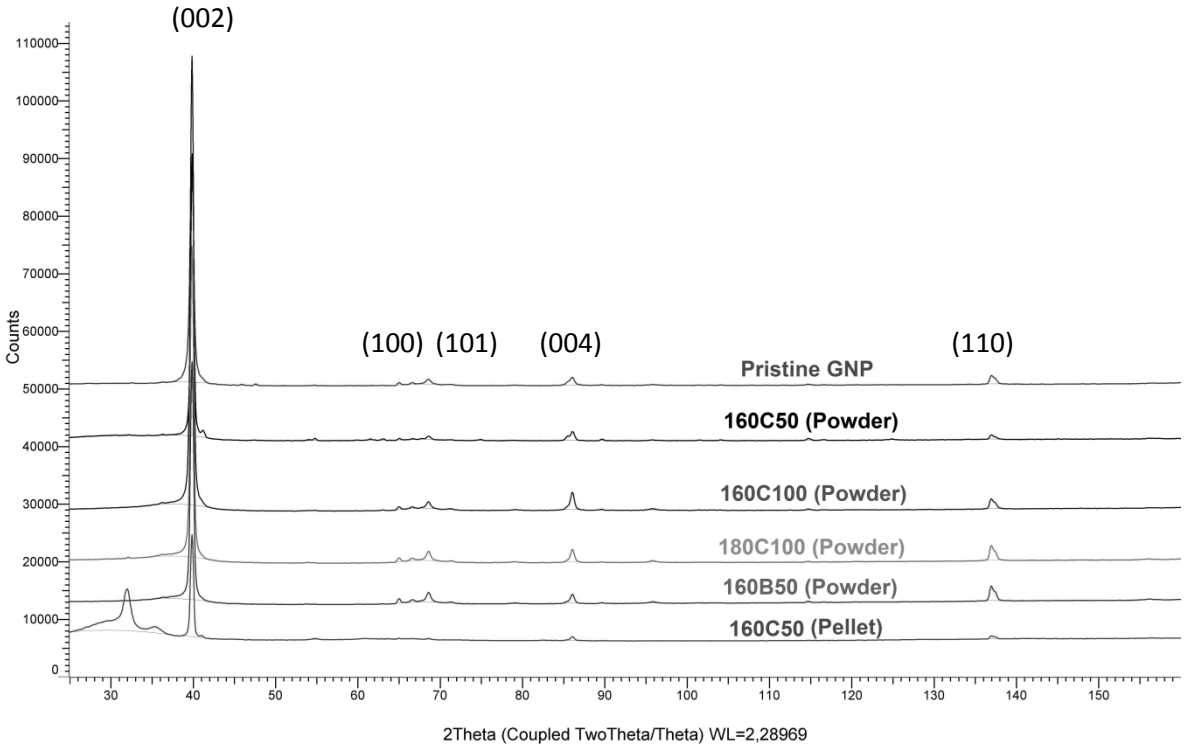

Figure 30. X-ray diffractograms of the pristine GNP powder, the fillers after different processing steps and the filled polymer extruded with the conventional screw at 50 rpm and 160 °C at 5 vol% filler content

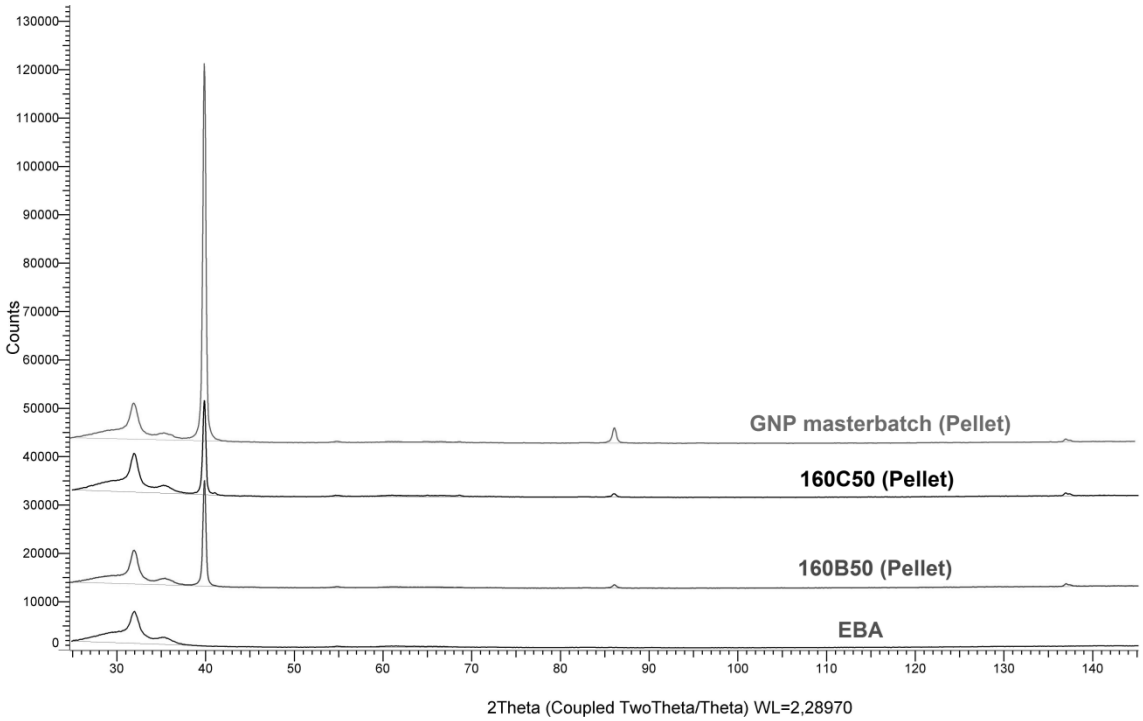

Figure 31. X-ray diffractograms of the pellets of EBA, pellets from the GNP masterbatch and the processed composites with the barrier and conventional screw (50 rpm, 160 °C and 5 vol% filler content).

4.6. Mechanical properties

The uniaxial tensile mechanical properties are shown in Figure 33 and Table 12. The stress–strain curves show the behavior of the EBA copolymer and the 11 vol% and 3.5 vol% hybrid filled systems. In the case of 11 vol% filled system, the curves for composites processed with the barrier screw and the conventional screw are compared.

The EBA copolymer had the lowest Young's modudus (128 MPa) and very good elastic (ductile) properties. Due to equipment restrictions, the elongation at break was not possible to determine for the composite materials containing 3.5 vol% filler and for the EBA, but in both cases an elongation of 800% was reached. For the same reason the ultimate strength was not determined. Young´s modulus (E) in the case of 3.5 vol% filler content double was that of the EBA with a value of 318 MPa. As expected, an increase on the stiffness of the material was observed with the addition of the rigid fillers with high aspect ratios.

In the case of 11 vol% filler, the elongation at break decreased sharply compared to that of the neat polymer as was expected. For the two differently processed materials the strain at break was approximately 70 %. The ultimate tensile strength (σ_b) was also similar for both materials and about 8 MPa. The E-modulus was increased further with higher amounts of filler taking a value of approximately 560 MPa in the case of the barrier screw and 540 MPa for the conventional screw. Thus there were no greater differences in mechanical behavior between those two composites. The reason for this could be the lack of adhesion between the platelets and the polymer.

The standard deviations for the experimental data are given in Table 12. As expected, because of its better dispersion capability, the properties obtained with the barrier screw exhibited lower values of the standard deviation than those from the conventional screw.

Table 12. Averages of Young´s modulus (E), ultimate strength (σ_b) and final elongation (ε_b) and standard deviations for neat EBA and systems with different hybrid filler contents processed with conventional and barrier extruder

		E (MPa)	σ_b (MPa)	ε_b (%)
EBA	Average	128	x	x
	Standard deviation	7	x	x
160C50 3.5 vol%	Average	318	x	x
	Standard deviation	18	x	x
160B50 11 vol%	Average	559	8,1	72
	Standard deviation	33	0,1	2,8
160C50 11 vol%	Average	539	8,1	71
	Standard deviation	51	0,2	20

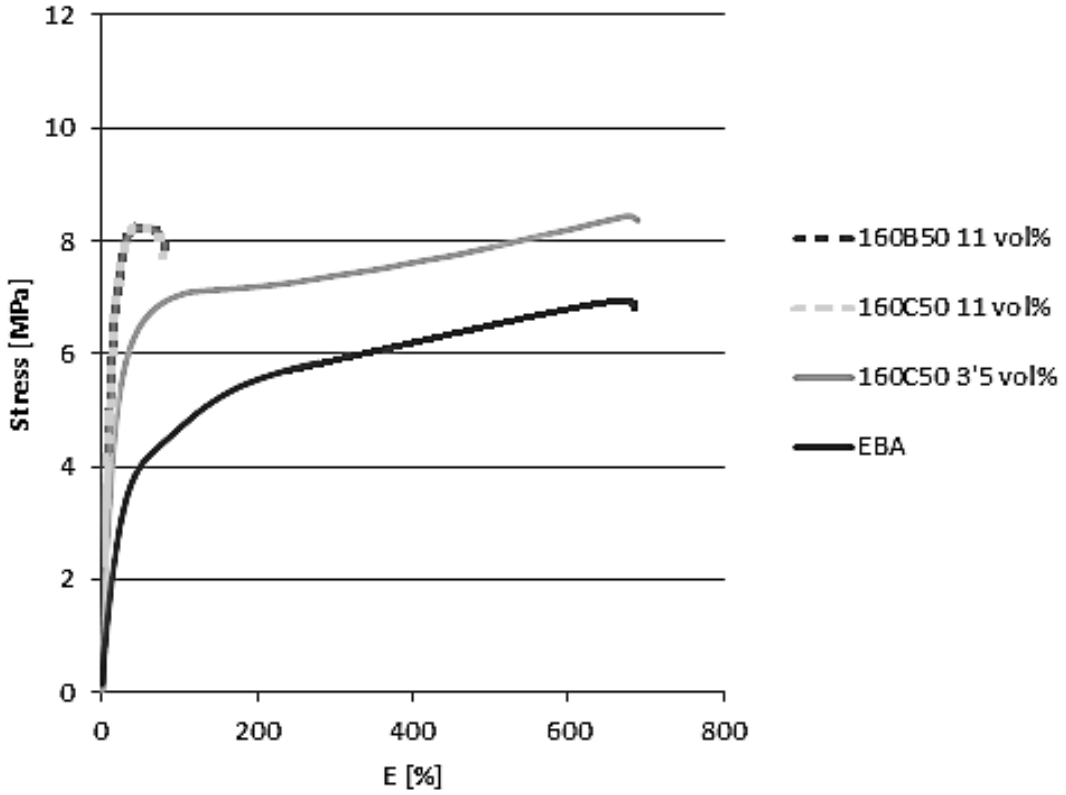

Figure 32 The mechanical properties of neat EBA and systems with different hybrid filler contents processed with the conventional and the barrier extruder. All samples were extruded at 50 rpm and 160°C

4.7. Rheological properties

Figure 34 shows the results from the viscosity measurements for the neat EBA and 11 vol% and 3.5 vol% filled systems. The viscosity was not very much affected by the presence of those quite low amounts of fillers, although it is clear that the viscosity increased with increasing filler content.

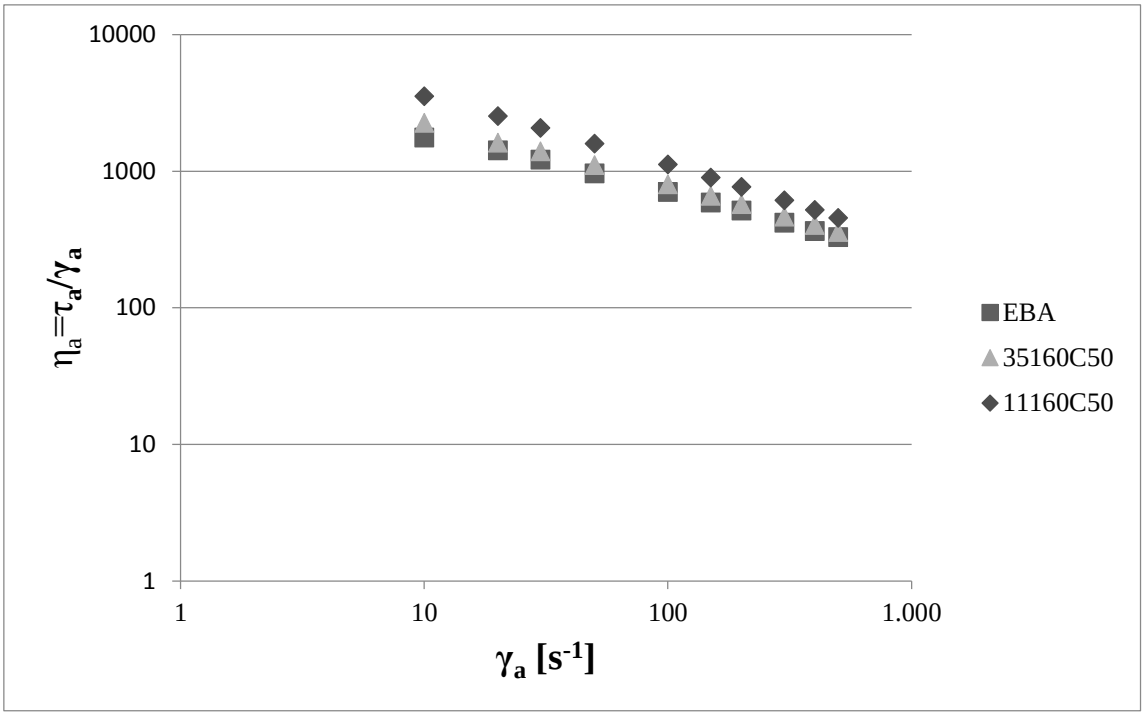

Figure 33. The apparent viscosity as a function of shear rate for neat EBA and composite melts processed with the conventional screw (3.5 and 11% hybrid fillers).

5. Conclusions

— The percolation curves of an EBA matrix filled only with GNP or CB and the same curve for the composite system with both fillers combined were determined. A synergistic effect on the electrical properties of the hybrid system GNP and CB was observed in this work, thus corroborating the results obtained by Oxfall et al [4].

— The effect of extrusion mixing with conventional and barrier screw (the last with a distributive mixer device incorporated) on the hybrid filled composite (CB/GNP 20-80 wt %) was studied with regard to the electrical properties. The percolation threshold for the specimens obtained with the conventional screw was lower than those obtained with the internal mixer. A beneficent microstructure could be the reason for these enhanced electrical properties. Morphological studies showed a low breakage of the platelets with the conventional screw, which could be one of the possible reasons for the low percolation threshold. Besides, a presence of thin and close agglomerates, usually in pairs, was observed. This introduces the suggestion of a possible de-agglomeration of the GNP corroborating the effect observed in the electrical conductivity. However, de-agglomeration could also have taken place during the compounding with twin screw of the masterbatches used in this work.

  The percolation threshold of specimens obtained with the barrier screw was higher than that observed with the internal mixer. This could be due to a destruction of the network caused by the high breakage of GNP observed through morphological characterization.

— The influence of extrusion temperatures and screw speeds was also studied in this work. The variation of the temperature from 160 C to 180 C showed no significant influence on the electrical conductivity of the materials. A change in the rotation speed of the screw from 50 to 100 rpm neither exhibited conclusive tendencies on the electrical properties. The effect of the change in shear stresses due to lower temperature or higher rotation speeds is therefore thought to be small within the ranges of temperatures and rotation speeds used in this work.

— The effect of an elongational flow on the electrical conductivity of the extruded hybrid composites with conventional and barrier screw was studied with the assistance of a capillary viscometer. The influence was detrimental in the materials extruded with the conventional screw (decreasing the electrical conductivity) whereas it was beneficial for those extruded with the barrier screw (increasing the conductivity). The accumulation of filler in the central region of the samples could be the reason behind the beneficial effect with the barrier screw whereas a higher orientation of the platelets is thought to be explanation for the detrimental effect with the conventional screw.

— Tensile tests were performed on the composites with different hybrid filler contents extruded with the conventional and the barrier screw. The mechanical properties were compared to those of the EBA copolymer also tested. An addition of 3.5% filler did not markedly affect the strain at break keeping it above 800% but doubled the Young's modulus with a value of 320MPa. In the case of 11 vol. % filler content, the elongation decreased sharply (to approximately 70 % of strain) compared to that of the neat polymer and the stiffness increased to approximately 560 MPa. The increase in stiffness was thought to be the consequence of the high aspect ratio combined with high stiffness of the graphite nanoplatelets.

The comparison of the mechanical properties between the materials processed with the conventional and the barrier screw showed no significant differences. The reason for this somewhat unexpected behavior could be the lack of adhesion between the platelets and the polymer seen through morphological characterization.

— The viscosities of composites with different hybrid filler contents extruded with conventional and barrier screws were also measured in this work. The viscosity was not very much affected by the presence of the amounts of fillers used here.

Appendix A

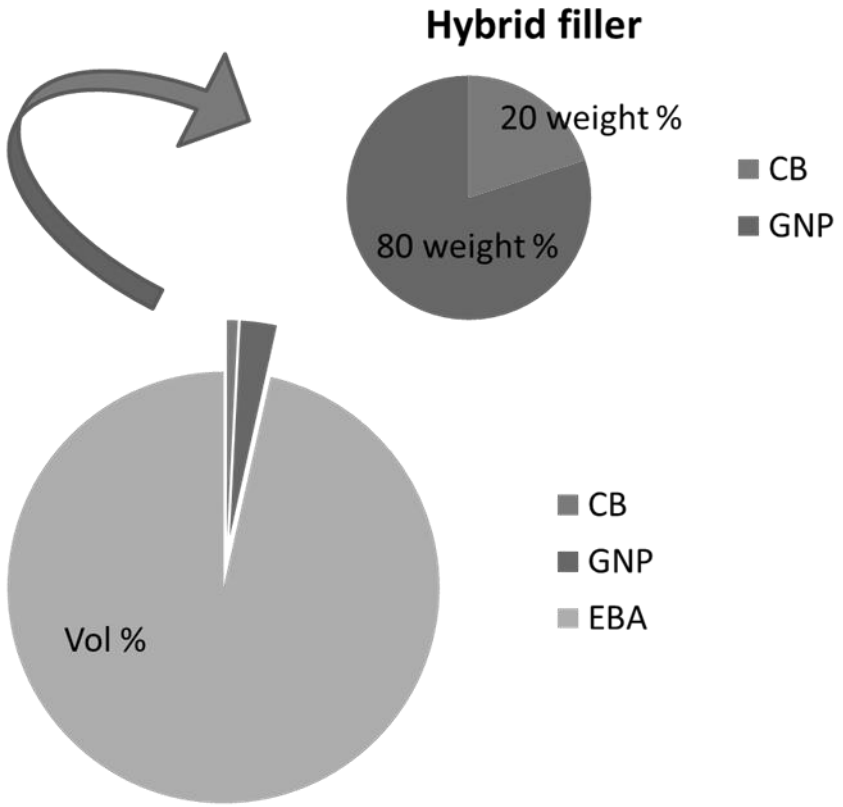

Figure 34. Graphical explanation of the composition in the hybrid filled polymer used in this work. The lower plot in is an illustrative representation of the proportions of polymer and filler. The upper plot shows the composition of the filler.

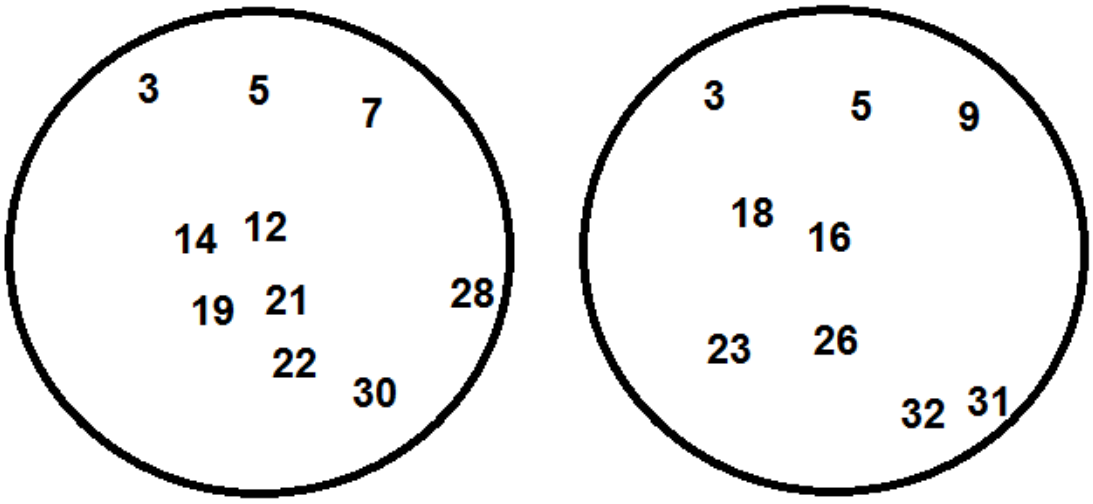

Figure 35. Schematic drawing of the location of the points of the taken pictures in the extrudates in Figures 23 (left) and 24 (right)

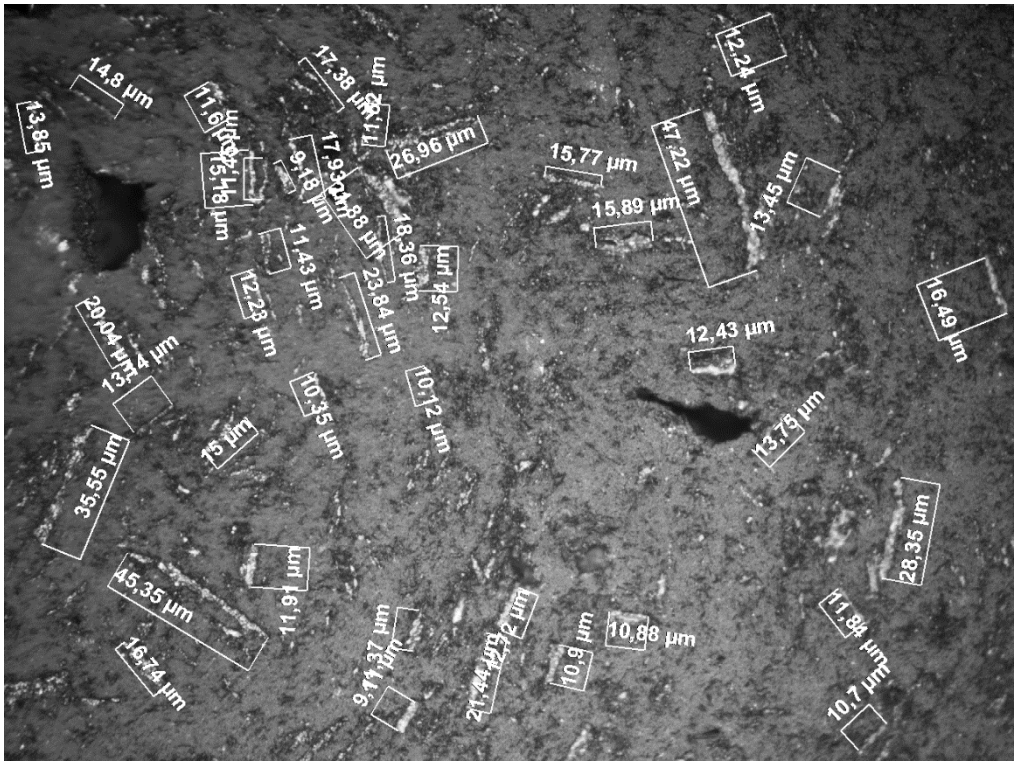

Figure 36 Example of the length analysis provided by the software AxioVision

Figure 37. Example of the area analysis provided by the software AxioVision.

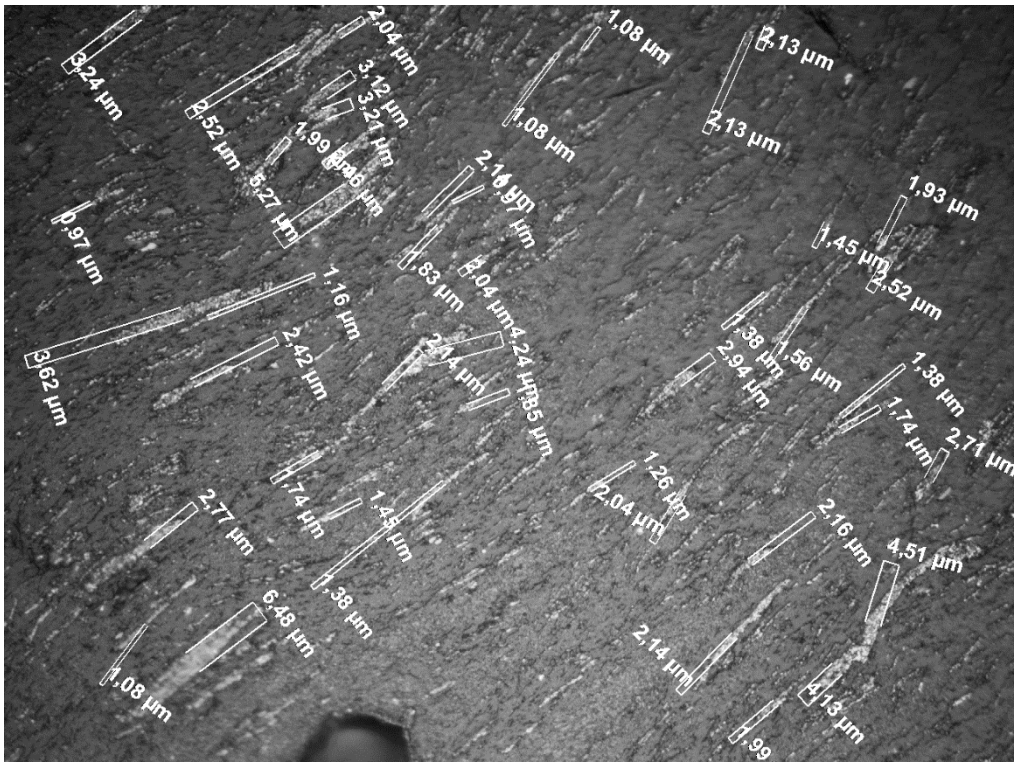

Figure 38. Example of the width analysis provided by the software AxioVision

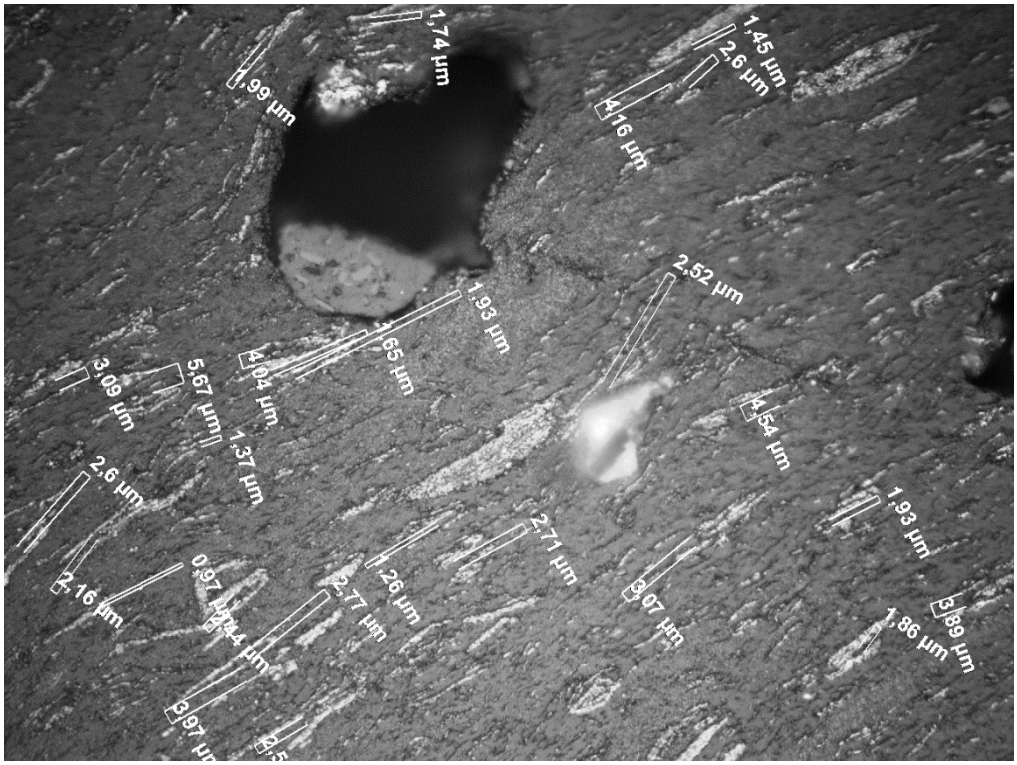

Figure 39 Example of the analysis of the separation distances provided by the sofware AxioVision.

References

[1] G. Mazzanti and M. Massimo, *Extruded Cables for High-Voltage Direct-Current Transmission: Advances in Research and Development*. Wiley-IEEE Press, 2013, p. 384.

[2] S. J. Han and J. Kjellqvist, "Fundamentals of Electrical Stress Control of Semiconductive Shield for Power Cables," in *62nd IWCS Conference*.

[3] K.-M. Jager and L. Lindbom, "The continuing evolution of semiconductor materials for power cable applications," *IEEE Electr. Insul. Mag.*, vol. 21, 2005.

[4] H. Oxfall, C. tekniska högskola, and C. tekniska högskola. D. of M. and M. Technology, *Manufacturing and Characterization of Filled Polymeric Systems: Powder Injection Moulding Feedstocks and Graphite Nanoplatelet Based Nanocomposites*. 2013.

[5] T. D. Fornes and D. R. Paul, "Formation and properties of nylon 6 nanocomposites," *Polímeros*, vol. 13, no. 4, pp. 212–217, Dec. 2003.

[6] D. V Rosato, M. G. Rosato, and D. V Rosato, *Concise encyclopedia of plastics*. 2000, p. 680.

[7] R. Chitta, R. Brüll, T. Macko, V. Monteil, C. Boisson, E. Grau, and A. Leblanc, "Characterization of Ethylene methyl methacrylate and Ethylene butylacrylate Copolymers with Interactive Liquid Chromatography," *Macromol. Symp.*, vol. 298, no. 1, pp. 191–199, Dec. 2010.

[8] "The Chemistry Of Polyethylene Insulation." [Online]. Available: http://www.lyondellbasell.com/techlit/techlit/Tech Topics/Equistar Industry Papers/Chemistry of PE Insulation.pdf. [Accessed: 01-Aug-2014].

[9] P. Nordell, "Alumiun Oxide-Poly (Ethylene-Co-Butyl Acrylate) Nanocomposites: synthesis, structure, transport properties and long-term performance," Kungliga Tekniska Högskolan, 2011.

[10] Y. J. Li, M. Xu, J. Q. Feng, X. L. Cao, Y. F. Yu, and Z. M. Dang, "Effect of the matrix crystallinity on the percolation threshold and dielectric behavior in percolative composites," *J. Appl. Polym. Sci.*, vol. 106, pp. 3359–3365, 2007.

[11] N. G. McCrum, C. P. Buckley, and C. B. Bucknall, *Principles of Polymer Engineering*. 1997.

[12] A. J. Brandolini and D. D. Hills, *NMR Spectra of Polymers and Polymer Additives*. 2000.

[13] Equistar, "Highly stabilized flame retarded polyolefin insulation compounds." [Online]. Available: http://www.lyondellbasell.com/techlit/techlit/Tech Topics/Equistar Industry Papers/Flame Retarded PE.pdf. [Accessed: 17-Aug-2014].

[14] M. El Hasnaoui, a. Triki, M. P. F. Graça, M. E. Achour, L. C. Costa, and M. Arous, "Electrical conductivity studies on carbon black loaded ethylene butylacrylate polymer composites," *J. Non. Cryst. Solids*, vol. 358, no. 20, pp. 2810–2815, Oct. 2012.

[15] T. Blythe and D. Bloor, *Electrical Properties of Polymers*. Cambridge University Press, 2005.

[16] J. J. George and A. K. Bhowmick, “Influence of Matrix Polarity on the Properties of Ethylene Vinyl Acetate-Carbon Nanofiller Nanocomposites.,” *Nanoscale Res. Lett.*, vol. 4, no. 7, pp. 655–664, Jan. 2009.

[17] R. C. B. Jean-Baptiste Donnet and M. J. Wang, *Carbon Black: Science and Technology, Second Edition*. CRC Press, 1993, p. 461.

[18] E. Bingham, B. Cohrssen, and C. H. Powell, *Patty’s Toxicology*. Hoboken, NJ, USA: John Wiley & Sons, Inc., 2001.

[19] “Cabot Carbon Black Glossary.” [Online]. Available: http://www.cabot-corp.com/wcm/sepdown/rd/cb/glossary_carbon.html. [Accessed: 01-Aug-2014].

[20] T. Ungár, J. Gubicza, G. Ribárik, C. Pantea, and T. W. Zerda, “Microstructure of carbon blacks determined by X-ray diffraction profile analysis,” *Carbon*. Elsevier, 15-Oct-2002.

[21] “Health and Hygiene - What is Carbon Black? - International Carbon Black Association,” 2014. [Online]. Available: http://www.carbon-black.org/index.php/what-is-carbon-black/health-and-hygiene. [Accessed: 01-Aug-2014].

[22] M. Inagaki and F. Kang, *Carbon Materials Science and Engineering: From Fundamentals to Applications*. 2006.

[23] “Bulk Graphene Nanoplatelets | World-Leading Graphene Company - XG SciencesWorld-Leading Graphene Company – XG Sciences.” [Online]. Available: http://xgsciences.com/products/graphene-nanoplatelets/. [Accessed: 01-Aug-2014].

[24] Y.-W. M. S.C. Tjong, “Physical Properties and Applications of Polymer Nanocomposites | 978-1-84569-672-6 | Elsevier.” [Online]. Available: https://www.elsevier.com/books/physical-properties-and-applications-of-polymer-nanocomposites/tjong/978-1-84569-672-6. [Accessed: 01-Aug-2014].

[25] Z. Fan, C. Zheng, T. Wei, Y. Zhang, and G. Luo, “Effect of carbon black on electrical property of graphite nanoplatelets/epoxy resin composites,” *Polym. Eng. Sci.*, vol. 49, no. 10, pp. 2041–2045, Oct. 2009.

[26] M. Sahini, *Applications Of Percolation Theory*. CRC Press, 2003, p. 276.

[27] K. Kalaitzidou, H. Fukushima, and L. T. Drzal, “A Route for Polymer Nanocomposites with Engineered Electrical Conductivity and Percolation Threshold,” *Materials*, vol. 3. pp. 1089–1103, 2010.

[28] O. Olabisi and K. Adewale, *Handbook of Thermoplastics*. 1997.

[29] E. V. Kuvardina, L. A. Novokshonova, S. M. Lomakin, S. A. Timan, and I. A. Tchmutin, “Effect of the graphite nanoplatelet size on the mechanical, thermal, and electrical properties of polypropylene/exfoliated graphite nanocomposites,” *J. Appl. Polym. Sci.*, p. n/a–n/a, Jul. 2012.

[30] J. Li and J.-K. Kim, “Percolation Threshold of Conducting Polymer Composites Containing 3D randomly Distributed Graphite Nanoplatelets,” *Compos. Sci. Technol.*

[31] A. Shenoy, *Rheology of filled polymer systems*. 1999.

[32] J. Leng, “Conductive Shape Memory Polymer Composite Incorporated with Hybrid Fillers: Electrical, Mechanical, and Shape Memory Properties,” *J. Intell. Mater. Syst. Struct.*, vol. 22, no. 4, pp. 369–379, Mar. 2011.

[33] P.-C. Ma, M.-Y. Liu, H. Zhang, S.-Q. Wang, R. Wang, K. Wang, Y.-K. Wong, B.-Z. Tang, S.-H. Hong, K.-W. Paik, and J.-K. Kim, “Enhanced electrical conductivity of nanocomposites containing hybrid fillers of carbon nanotubes and carbon black.,” *ACS Appl. Mater. Interfaces*, vol. 1, no. 5, pp. 1090–6, May 2009.

[34] J. Chen, X.-C. Du, W.-B. Zhang, J.-H. Yang, N. Zhang, T. Huang, and Y. Wang, “Synergistic effect of carbon nanotubes and carbon black on electrical conductivity of PA6/ABS blend,” *Compos. Sci. Technol.*, vol. 81, pp. 1–8, Jun. 2013.

[35] T. Wei, L. Song, C. Zheng, K. Wang, J. Yan, B. Shao, and Z.-J. Fan, “The synergy of a three filler combination in the conductivity of epoxy composites,” *Mater. Lett.*, vol. 64, no. 21, pp. 2376–2379, Nov. 2010.

[36] N. . Enikolopyan, M. Fridman, I. O. Stalnova, and V. L. Popov, “Filled polymers: Mechanical properties and processability,” *Adv. Polym. Sci.*, 1990.

[37] Y.-W. Mai and Z.-Z. Yu, *Polymer nanocomposites*. Boca Raton, FL :: CRC Press ;, 2006.

[38] N. P. Cheremisinoff and P. N. Cheremisinoff, *Elastomer Technology Handbook*. CRC Press, 1993, p. 1120.

[39] S. Ahmed Salahudeen, R. H. Elleithy, O. AlOthman, and S. M. AlZahrani, “Comparative study of internal batch mixer such as cam, banbury and roller: Numerical simulation and experimental verification,” *Chem. Eng. Sci.*, vol. 66, no. 12, pp. 2502–2511, Jun. 2011.

[40] J. F. I. Housz and H. E. H. Meijer, “The melting performance of single screw extruders,” *Polym. Eng. Sci.*, vol. 21, no. 6, pp. 352–359, Apr. 1981.

[41] “Single-Screw Mixing 101 : Plastics Technology.” [Online]. Available: http://www.ptonline.com/columns/single-screw-mixing-101. [Accessed: 24-Aug-2014].

[42] R. Arino and A. Boldizar, “Barrier screw compounding and mechanical properties of anethylene-acrylic acid copolymer and cellulose fiber composite,” *Int. Polym. Process.*, 2013.

[43] R. Arino and A. Boldizar, “Melt Processing of Wood Cellulose Tissue and Ethylene-Acrylic Acid Copolymer Composites,” *Int. Polym. Process.*, 2013.

[44] S. J. Han and W.-K. Lee, “Semiconducting Shield Compositions. United States Patent No.: US 6455771 B1,” 2002.

[45] V. Haddadi-Asl, M. Kazacos, and M. Skyllas-Kazacos, “Carbon–polymer composite electrodes for redox cells,” *J. Appl. Polym. Sci.*, vol. 57, no. 12, pp. 1455–1463, Sep. 1995.

[46] R. M. Kulkarni, H. N. Narasimha Murthy, G. B. Rudrakshi, and M. Prathap, “Parametric Study of Twin Screw Extrusion for Processing Epoxy/Carbon Black Nanocomposites Using Orthogonal Array Technique,” *Journal of Polymer & Composites*, vol. 1, no. 2. pp. 15–26.

[47] G. Ariu, “Influence of low-structure carbon black on the electrical, rhological and mechanical properties of graphite nanoplatelets/ethyl butyl acrylate composites,” Chalmers University of Technology, 2013.

[48] M. Inagaki, *New Carbons - Control of Structure and Functions*. Elsevier, 2000, p. 240.